THE EFFECT OF DIABETES ON RAT SKELETAL MUSCLE TISSUES AT MOLECULAR LEVEL

A THESIS SUBMITTED TO
THE GRADUATE SCHOOL OF NATURAL AND APPLIED SCIENCES
OF
MIDDLE EAST TECHNICAL UNIVERSITY

BY

ÖZLEM BOZKURT

IN PARTIAL FULFILLMENT OF THE REQUIREMENTS
FOR
THE DEGREE OF MASTER OF SCIENCE
IN
BIOLOGY

SEPTEMBER 2006

Approval of the Graduate School of Natural and Applied Sciences.

Prof. Dr. Canan ÖZGEN
Director

I certify that this thesis satisfies all the requirements as a thesis for the degree of Master of Science.

Prof. Dr. Semra Kocabıyık
Head of Department

This is to certify that we have read this thesis and that in our opinion it is fully adequate, in scope and quality, as a thesis for the degree of Master of Science.

Prof. Dr. Feride Severcan
Supervisor

Examining Committee Members

Prof. Dr. İnci Togan	(METU, BIO)	
Prof. Dr. Feride Severcan	(METU, BIO)	
Assoc. Prof. Dr. Ewa Doğru	(METU, BIO)	
Assoc. Prof. Dr. Mehmet Dinçer Bilgin	(ADU, Biophys.)	
Assist. Prof. Dr. Neslihan Toyran Al-Otaibi	(BU, Physiol.)	

I hereby declare that all information in this document has been obtained and presented in accordance with academic rules and ethical conduct. I also declare that, as required by these rules and conduct, I have fully cited and referenced all material and results that are not original to this work.

Name, Last name : Özlem Bozkurt
Signature :

ABSTRACT

THE EFFECT OF DIABETES ON RAT SKELETAL MUSCLE TISSUES AT MOLECULAR LEVEL

BOZKURT, Özlem

M.Sc., Department of Biology

Supervisor: Prof. Dr. Feride SEVERCAN

September 2006, 86 pages

In the present study Fourier Transform Infrared Spectroscopy was used to examine the effects of streptozotocin-induced diabetes mellitus on the structural components of slow- and fast-twitch rat skeletal muscles, at molecular level.

Diabetes mellitus is a chronic disorder of carbohydrate, fat and protein metabolism, which is characterized by hyperglycemia caused by a defective or deficient insulin secretory response. The effect of diabetes is seen on a variety of tissues leading to important secondary complications such as kidney failure, liver dysfunction, cardiac disorders, etc. Skeletal muscle is one of the major tissues determining carbohydrate and lipid metabolism in the body; therefore, is one of the target tissues of diabetes. The two main types of muscle fibers are type I (slow-twitch) and type II (fast-twitch) fibers; having different structural organization and metabolic features.

The FTIR spectra revealed a considerable decrease in lipid and protein content of diabetic skeletal muscles, indicating an increased lipolysis and protein breakdown or decreased protein synthesis. Moreover changes in protein structure and conformation were observed. In diabetes, muscle membrane lipids were more ordered and the amount of unsaturated lipids was decreased possibly due to lipid peroxidation. Diabetes caused a decrease in the content of nucleic acids, especially RNA, and hydrogen bonded phospholipids in the membrane structures of skeletal muscles.

In all of the spectral parameters investigated slow-twitch muscle was more severely affected from diabetes. Thus, FTIR spectroscopy appears to be a useful method to evaluate the effect of diabetes on skeletal muscle tissues at molecular level.

Key words: FTIR spectroscopy, diabetes, skeletal muscle, skeletal muscle fiber types

ÖZ

DİYABETİN SIÇAN İSKELET KAS DOKULARI ÜZERİNDEKİ ETKİLERİNİN MOLEKÜLER DÜZEYDE İNCELENMESİ

BOZKURT, Özlem

Yüksek Lisans, Biyoloji Bölümü
Tez Yöneticisi: Prof. Dr. Feride Severcan

Eylül 2006, 86 sayfa

Bu çalışmada streptozotocin enjeksiyonu ile oluşturulan diabetes mellitus hastalığının yavaş ve hızlı kasılan iskelet kasları üzerindeki etkisi Fourier Dönüşüm Kızılötesi Spektroskopisi (FTIR) ile moleküler düzeyde incelenmiştir.

Diabetes mellitus karbonhidrat, yağ ve protein metabolizmasını etkileyen kronik bir hastalıktır, ve yetersiz insulin salgılanmasından kaynaklanan hiperglisemi ile tanımlanmaktadır. Diyabetin etkileri pek çok dokuda görülür ve neden olduğu önemli komplikasyonlar arasında kalp ve böbrek yetmezliği, karaciğer bozuklukları sayılabilir. İskelet kası karbonhidrat ve lipid metabolizmasını belirleyen başlıca dokular arasında yer aldığından diyabetten en fazla etkilenen dokulardandır. Yapısal organizasyonu ve matabolik özellikleri birbirinden farklı iki ana kas lifi çeşidi vardır: tip I (yavaş kasılan) ve tip II (hızlı kasılan).

FTIR sonuçları diyabetik iskelet kaslarında artmış lipoliz ve protein yıkımı ya

da azalmış protein sentezini gösteren lipid ve protein içeriğinde önemli bir azalma tespit etmiştir. Ayrıca protein yapısı ve konformasyonunda değişiklikler gözlenmiştir. Diyabette, kas membrane lipidlerinin daha düzenli olduğu ve doymamış lipid miktarında, muhtemelen lipid peroksidasyonundan kaynaklanan, bir artış olduğu gösterilmiştir. Diyabet iskelet kaslarında nükleik asit miktarında, özellikle RNA miktarında, ve membrane yapısındaki hidrojen-bağlı fosfolipidlerin miktarında azalmaya neden olmuştur.

İncelenen bütün spektral parametreler yavaş kasılan iskelet kas dokusunun diyabetten daha çok etkilendiği bulunmuştur. Sonuç olarak, FTIR spektroskopisi diyabetin iskelet kas dokuları üzerindeki etkilerini moleküler düzeyde incelemek için kullanışlı bir araç olarak görünmektedir.

Anahatar Kelimeler: FTIR spektroskopisi, diyabet, iskelet kası, iskelet kas lifi çeşitleri

To my mother,

ACKNOWLEDGEMENTS

I would like to thank to my supervisor Prof. Dr. Feride SEVERCAN for her guidance, patience, encouragement and supervision throughout this thesis study.

I would also like to thank to Assos. Prof. Mehmet Dinçer BİLGİN for his suggestions and guidance with the animal studies.

I also compassionately express my special thanks to Sevgi Görgülü and Emel Özkan owing to their precious help and lovely attitude in the course of experimental period and writing this thesis.

I would like to thank to Banu Akkaş, Havva Dinç and my labmates, for their sincere friendship and supports.

I would like to send my ultimate appreciation to my mother Asiye Bozkurt, my brother Cem Taylan Bozkurt and my sister Bilge Bozkurt Cansevgisi, and also to Can Sarısözen for their endless patience, encouragement, support and love.

TABLE OF CONTENTS

LIST OF FIGURES

FIGURES

LIST OF TABLES

TABLES

CHAPTER 1

INTRODUCTION

In this study the effects of Streptozotocin (STZ)-induced type I diabetes on two types of skeletal muscles, namely Soleus (SOL) and Extensor Digitorum Longus (EDL) were reported at molecular level via Fourier transform infrared (FTIR) spectroscopy. In this chapter a detailed preliminary survey including structural properties of skeletal muscle, types of skeletal muscles and their structural properties, diabetes mellitus, the effects of diabetes mellitus on skeletal muscle tissue, and basis of infrared spectroscopy have been conducted.

1.1 Skeletal Muscle

Skeletal muscle comprises a large percentage of the body mass. They are an elegant assembly of contractile proteins and their supporting membranes and organelles. Skeletal muscles are usually attached to bones, and are called striated owing to their appearance under the microscope. They contract voluntarily, and they can develop great power but run for short periods of time (Greisheimer and Wiedeman, 1972). Muscle development and normal activity are dependent on and closely integrated with the central and peripheral nervous systems, which together contribute to the motor unit. A motor unit is composed of a motor neuron in the brain stem or spinal cord; the peripheral axon emanating from the motor neuron; the neuromuscular junction; and finally the skeletal muscle fiber (Kumar, Cotran and Robbins, 1997).

1.1.1 Structural Organization of Skeletal Muscle

Skeletal muscle has a complex organization composed of lines of connective tissue covering parallel bundles of long cylindrical cells called fibers. The structural organization of muscle and muscle fibers is shown in Figure 1. A fibrous connective tissue called the epimysium, surrounds the entire muscle. This is a protective sheet joining the intramuscular tissue to form a dense, strong connective tissue of the tendons. The tendons connect both ends of the muscle to outermost covering of bones. Under epimysium, there are bundle of many fibers constituting the fasciculi. The partitions of connective tissue extending from epimysium, which surround the fasciculi, are called perimysium. A fine layer of connective tissue, which further covers each muscle fiber and separates it from neighboring fibers, is called the endomysium. Capillaries form a network within the endomysium supplying oxygen and nutrients to individual muscle fibers. Beneath the endomysium, the double-layered, thin and elastic cell membrane lie which is called sarcolemma. It contains a plasma membrane which is a bilayer of lipids, and a basement membrane which contains proteins and strands of collagen. The cytoplasm of muscle fiber is called sarcoplasm, which contains enzymes, fat and glycogen particles, nuclei, mitochondria and other organelles. Each fiber has many nuclei, arranged around the peripheral part of the fiber. Sarcoplasmic reticulum, an extensive longitudinal lattice-like network of tubular channels and vesicles, allows the wave of depolarization to spread rapidly from the fiber's outer surface to its inner environment through the T-tubule system.

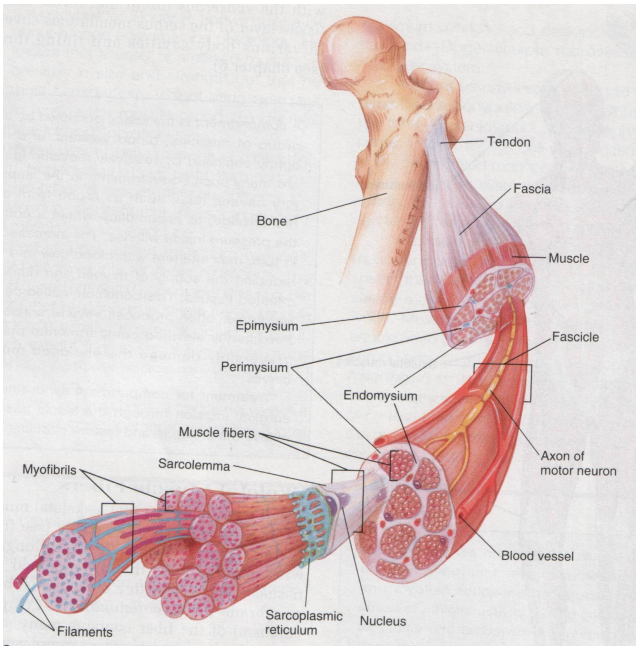

Figure 1. The structural organization of skeletal muscle (Shier *et al.*, 1996).

Water constitutes approximately 75% of skeletal muscle, and about 20% of skeletal mass is composed of proteins. Most abundant skeletal muscle proteins are myosin, actin and tropomyosin, which take role in muscle contraction. Also the oxygen binding protein, myoglobin, is found in skeletal muscle tissue. The remaining 5 % is composed of enzymes, salts, minerals, and other substances, including high-energy phosphates, urea, lactate, calcium, magnesium, phosphorous, sodium, potassium, chloride ions, amino acids, fats and carbohydrates (Greisheimer and Wiedeman, 1972; Shier *et al.*, 1996; McArdle, Katch, Katch, 2001).

1.1.2 The Structure of Sarcolemma and Muscle Contraction

A single multinucleated muscle fiber contains smaller functional units that lie parallel to the fibers long axis. These fibrils or myofibrils are composed of filaments or myofilaments, which consists of ordered assemblies of actin and myosin. Although actin and myosin are the major proteins that account for 85% of myofibrillar complex, there are other proteins found in the structure of myofibrils, namely tropomyosin, troponin, α-actitin, β-actinin, M protein and C protein.

In the structure of myfibrils there are cross-striations or alternating light and dark bands that constitute the striated nature of skeletal muscle. Owing to the appearance of myofibrils with polarized light, the dark bands were designated as A (anisotropic) and the light bands were designated as I (isotropic). The darker A bands are composed of thick myosin filaments and the lighter I bands are composed of the thin actin filaments. The thin dark line that bisects I bands and adheres to the sarcolemma is called as Z line, which gives stability to entire structure. The center of A bands contain the clear H zone or band, a region of lower optical activity due to the absence of actin filaments. The M band bisects the central portion of the H band, which shows the center of the Z lines, consisting of protein structures that support the arrangement of the myosin filaments. The sarcomere is the functional unit of skeletal muscle, which consists of basic repeating units between two Z lines (McArdle, Katch, Katch, 2001; Greisheimer and Wiedeman, 1972; Garrett *et al.*, 1983). The schematic representation of organization of myofibrils is shown in Figure 2, and the structure of a sarcomere is shown in Figure 3.

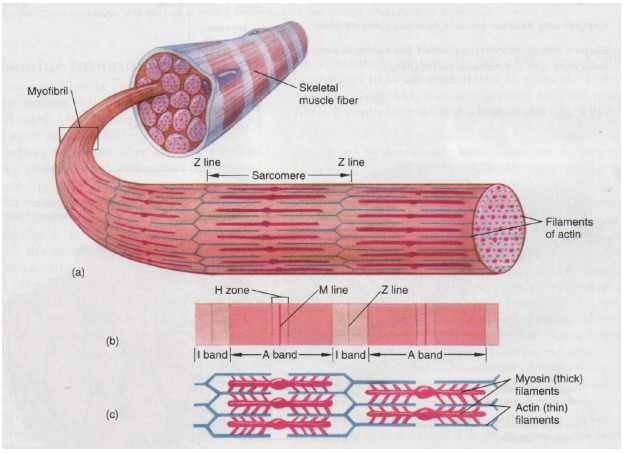

Figure 2. Organization of myofibrils (Shier *et al.*, 1996).

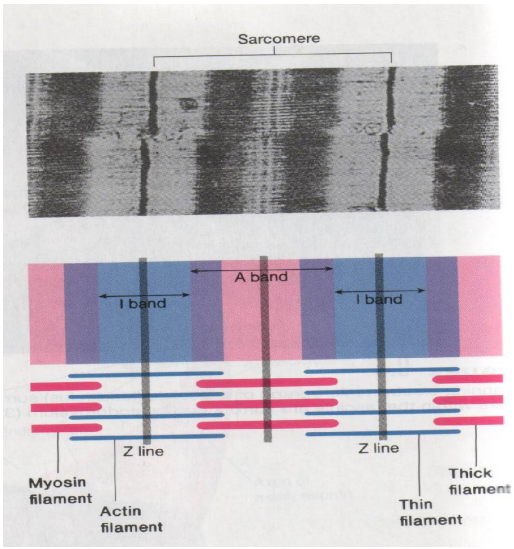

Figure 3. A sarcomere (Shier *et al*., 1996).

The sliding filament model proposed in 1950s, explain the mechanism of muscle contraction. The model proposes that a muscle shortens or lengthens due to the thick and thin filaments slide over each other, without actually changing the length. The myosin crossbridges, which cyclically attach, rotate and detach from the actin filaments with energy from ATP hydrolysis, provide the molecular motor to drive fiber shortening. This causes a major conformational change in relative size within the sarcomere's zones and bands. During contraction as myosin filaments slide on actin filaments, actin filaments are pulled towards the center of sarcomere meaning that I bands get shortened, Z bands are pulled towards the center of the sarcomere, H band gets smaller or can even disappear. However, as myosin and actin filaments get over each other they are recognized as dark bands, therefore; no change occurs in the length of A band (Shier *et al*., 1996).

1.2 Types of Skeletal Muscle Fibers

Skeletal muscle is composed of different fiber types, which are classified by their contractile and metabolic characteristics (Nemeth and Pette, 1981). The general classification of muscle fibers is as type I and type II skeletal muscle fibers. Type I and type II fibers have different levels of metabolic enzymes and contractile proteins (Okumura *et al.*, 2005). These fibers can be distinguished

by special stains for specific enzymes, enzymes that take role in oxidative or glycolytic metabolism of fuels inside skeletal muscle structure.

1.2.1 Type I (Slow-twitch) Fibers

Type I fibers are red fibers which are slow-contracting (slow-twitch), and oxidative. They are also named as slow oxidative fibers. Different skeletal fiber types can be distinguished by their enzymatic characteristics of myosin ATPase activity and molecular species of myosin heavy chain (MHC) isoforms. Type I fibers have low myosin ATPase activity (Garrett *et al.*, 1983), and they express type I MHC (Schiaffino and Reggiani, 1996; Okumura *et al.*, 2005). Also type I and type II fibers express different isoforms of myosin light chain (MLC) (Schiaffino and Reggiani, 1996). Delp *et al.* (1996) have shown that type I fibers have high citrate synthase activity, which is an indicator of oxidative metabolism. Therefore, type I fibers are better adapted to oxidative mechanism and have high oxidative enzyme systems. They are resistant to fatigue having a slower contraction time due to the slower calcium handling ability and shortening speed (McArdle, Katch, Katch, 2001). Therefore, they are best adapted for prolonged activity of relatively low intensity. Type I fibers have numerous transversely disposed mitochondria, a thick Z disc that contain five striations, and relatively low levels of sarcoplasmic reticulum and they have a bulkier sarcomere (Garrett *et al.*, 1983; Calore *et al.*, 2002). Type I fibers display an even granule deposition throughout their cross-sectional areas, showing that they have a smaller amount of glycogen (Armstrong *et al.*, 1975; Garrett *et al.*, 1983). Type I fibers are primarily used in submaximal endurance exercise, in contrast type II fibers are selectively used for exercises performed at intensities above the aerobic threshold (Gollnick *et al.*, 1974; Garrett *et al.*, 1983).

1.2.2 Type II (Fast-twitch) Fibers

Type II fibers are white and fast-contracting (fast-twitch) fibers. They are further divided into two groups as fast-contracting glycolytic (type IIB) and fast-contracting oxidative-glycolytic (type IIA) muscle fibers. They have high

myosin ATPase activity (Engel, 1962; Garrett *et al.*, 1983), and they express type IIa and IIb MHC depending on muscle fiber subtypes (Schiaffino and Reggiani, 1996; Okumura *et al.*, 2005). They have a higher concentration of enzymes involved in glycogen metabolism; therefore, have a better developed anaerobic energy system. It has been demonstrated that fast-contracting fibers had a higher phosphofructokinase (PFK) activity, which is an indicator of glycolytic action (Armstrong and Ianuzzo, 1977). They have faster contraction times, are less fatigue resistant. They are better adapted for intense activity in short period of time. The membrane specializations of the transverse tubular system are more highly developed ultrastructurally in type II fibers when compared with type I fibers (Garrett *et al.*, 1983). Type II fibers have a more streamlined sarcomere with a better developed membrane system for the rapid transmission of impulses in to the fiber. Hence, they have high capacity of electrochemical transmission of action potentials due to rapid Ca^{2+} release and uptake by an efficient sarcoplasmic reticulum (McArdle, Katch, Katch, 2001).

Type IIA fibers have a high oxidative potential than type IIB fibers, but lower than type I fibers. The contraction times of both type IIA and IIB are both faster than type I. Moreover, type IIA fibers are more resistant to fatigue than type IIB fibers (Burke *et al.*, 1973; Garrett *et al.*, 1983). Type IIB fibers have few mitochondria that are transversely disposed, a thin Z disc and abundant sarcoplasmic reticulum. Type IIA fibers have numerous longitudinal mitochondria, an intermediate Z disc and an intermediate content of sarcoplasmic reticulum (Calore *et al.*, 2002). Type II fibers have numerous electron dense granules throughout the cytoplasm, which are composed of glycogen.

1.3 Diabetes Mellitus (DM)

Diabetes mellitus (DM) is a chronic disorder of carbohydrate, fat and protein metabolism, which affects a large number of people of all social conditions throughout the world. A defective or deficient insulin secretory response, which translates into impaired carbohydrate (glucose) use, is a characteristic feature of DM, as is the resulting hyperglycemia. Therefore, in untreated state

DM is recognized by chronic elevation of glucose level in blood. This is sometimes accompanied by symptoms of severe thirst, profuse urination, weight loss, etc. The high concentration of blood glucose and other biochemical abnormalities results from a deficiency in β-cells of endocrine pancreas and/or from a sub sensitivity to insulin in target cells. Exact etiology of diabetes mellitus has not been established yet. Although there are several diseases and syndromes associated with hyperglycemia, it has been traditional to classify all forms of diabetes as either insulin-dependent (IDDM) or noninsulin-dependent (NIDDM) on functional grounds (Öztürk *et al*, 1997, Kumar, Cotran and Robbins, 1997).

1.3.1 Insulin-Dependent Diabetes Mellitus (IDDM)

Insulin, a peptide hormone, is secreted by the β-cells in response to a rise in blood glucose levels. Insulin or agents that can mimic its action are necessary to promote the entry of glucose into tissues where the glucose can either be converted into energy or stored for later use. In addition to glucose uptake, insulin regulates a variety of other metabolic responses, including facilitating entry of amino acids into cells for the production of cellular proteins, increasing precursors for nucleic acid synthesis, transporting critical cellular ions, stimulating Na^+/K^+ ATPase as well as controlling the expression of a number of genes (Stapleton, 2000). Insulin also regulates the transcription of the genes for several key enzymes associated with carbohydrate and fatty acid metabolism (O'Brien and Granner, 1996). Glycogen synthase (Shepherd, *et al.*, 1995), glucokinase (Magnuson *et al.*, 1989), phosphoenolpyruvate carboxykinase (PEPCK) (Short *et al.*, 1986, O'Brien *et al.*, 1990), fatty acid synthase (Stapleton *et al.*, 1990, Moustaid *et al.*, 1994) and glucose-6-phosphate dehydrogenase (Wagle *et al.*, 1998), key enzymes in glycogen synthesis, glycolysis, gluconeogenesis, fatty acid biosynthesis and pentose phosphate pathway, respectively, have been targets of the studies with regard to insulin action. The lack of critical concentrations of circulating insulin or the ability of insulin to function properly leads to the onset of diabetes mellitus (DM). In the untreated state, DM is recognized by chronic elevation of glucose in the blood. The high concentration of blood glucose and other biochemical

abnormalities results from a deficiency in β-cells of endocrine pancreas and/or from a sub-sensitivity to insulin in target cells. Although there are several diseases and syndromes associated with hyperglycemia, it has been traditional to classify all forms of diabetes as either insulin-dependent (IDDM) or noninsulin-dependent (NIDDM) on functional grounds (Öztürk *et al.*, 1997). IDDM usually begins before the age of 40, often in childhood and adolescence, and it results from a severe, absolute lack of insulin caused by a reduction in β-cell mass.

The clinical picture is usually more severe in patients with IDDM than in patients with NIDDM. Characteristically, the plasma insulin is low or immeasurable, because a total deficiency in pancreatic β-cells has occurred in IDDM. Three interlocking mechanisms are responsible for the islet cell destruction; they are genetic susceptibility, autoimmunity and an environmental result. The genetic susceptibility is related with the class II antigens of major histocompatibility complex. The altered antigen belonging to this group may bind to normal β–cells presenting them as abnormal cells to be destroyed to T-cells. Autoimmunity occurs in IDDM due to the T cell-mediated destruction of pancreatic β–cells. The environmental factors include viral infection in which a part of a viral protein very resembles a protein in pancreatic tissue that takes role in T-cell recognition. Moreover the viral infection may cause the altered DNA expression or DNA structure of some proteins in pancreas. When taken together viral infection leads to immune response against normal β–cells or against altered β–cells by damaging them (Kumar, Cotran and Robbins, 1997). In IDDM glucagon level is elevated, but it can be suppressible with insulin. This type of diabetes is not responsive to the treatment with oral antidiabetic drugs. Therefore, insulin therapy is always required for patients with IDDM. Autoimmune reactions seem to be quite possible for the pancreatic β-cell destruction, and the activation of cytokines such as interleukin-1 (IL-1) and tumor necrosis factor (TNF) may play an important role in this process (Mandrup-Poulsen, 1990; Rabinovitch and Baquerizo, 1990).

1.3.2 Noninsulin-Dependent Diabetes Mellitus (NIDDM)

This form of diabetes usually begins in middle life or after and the symptoms begin more gradually than in IDDM so the diagnosis is frequently made when an asymptomatic person is found to have elevated plasma glucose on routine laboratory examination. In contrast to IDDM, plasma insulin levels are normal to high in absolute term, although they are lower than predicted for the level of the plasma glucose, i.e., relative insulin deficiency is present. Insulin resistance seen in NIDDM involves both a decreased number of insulin receptors in target tissues and a postreceptor defect that has not been well identified, yet. Changes in the insulin receptor tyrosine kinase activity (Slieker *et al.*, 1990; Block *et al.*, 1991) and/or insulin sensitive glucose transporter (Garvey *et al.*, 1989, Strout *et al.*, 1990) may be the responsible mechanism(s) for the subsensitivity of target cells to insulin.

Although these types of patients are responsive to the treatment with oral antidiabetic drugs, many of them are treatable with diet and exercise alone. However in some cases treatment with combination of oral antidiabetic drugs and insulin is required (Knip and Akerblom, 1998).

1.3.3 Complications of Diabetes Mellitus:

The metabolic disturbances of DM cause chronic, irreversible damage to vital organs and systems. Most of the available experimental and clinical evidence suggests that the complications of diabetes results from metabolic derangements, mainly hyperglycemia (Kumar, Cotran and Robbins, 1997).
Various short-term and long-term complications may occur in diabetic patients. These complications can be categorized as neurological, cardiovascular, gastrointestinal, urological, respiratory, ophthalmic, reproductive, haematological, biochemical complications and complications related to drug metabolism and pharmacokinetics. Certain diabetic complications such as gastroenteropathy or the development of urinary bladder dysfunction are not fatal in nature, although they may seriously affect the quality of life in diabetic patients. However some of the diabetic complications like neuropathy, nephropathy, angiopathy and cardiomyopathy may be deleterious for diabetic

patients; development of these complications has been shown to confer an increased incidence of morbidity and mortality of diabetic patients (Öztürk *et al.*, 1997).

1.3.4 Oxidative Stress in Diabetes Mellitus

Long-term pathology of diabetes occurs as a consequence of persistent hyperglycemia. Four consequence of hyperglycemia of particular pathological relevance are the formation, auto-oxidation, and interaction with cell receptors of advanced glycation end products (AGEs); activation of various isoforms of protein kinase C; induction of the polyol pathway; and increased hexosamine pathway flux. Many of these pathways have long been associated with elevated oxidative stress (Green *et al.*, 2004).

Enhanced oxidative stress and changes in antioxidant capacity are considered to play an important role in the pathogenesis of chronic diabetic complications (Baynes, 1991). Evidence indicates that free oxygen radicals and membrane lipid peroxidation are significantly increased in diabetic patients and in experimental diabetic rats (Altomare *et al.*, 1992; Severcan *et al.*, 2005). Increased oxidative stress, which contributes to the pathogenesis of diabetic complications, is the consequence of either enhanced ROS production or attenuated ROS scavenging capacity, resulting in tissue damage that in most instances is assessed by the measurement of lipid peroxides (Halliwell and Gutteridge, 1989; West, 2000).

Mitochondria constantly generate reactive oxygen species (ROS), which can damage their lipids, proteins, DNA and RNA. Diabetes-induced mitochondrial dysfunction may contribute to diabetes-associated pathology. Mitochondrial dysfunction may also contribute to diabetic complications by producing potentially toxic free radicals and diffusible prooxidants. The respiratory chain, responsible for a constant generation of ROS within the cell, is located mostly within the inner mitochondrial membrane. Unlike most biological membranes, this membrane is extremely rich in proteins, which make up more than 80% of its dry weight. Owing to this unique feature, inner membrane proteins are

primary targets for oxidative damage induced by mitochondrial generated ROS (Netto *et al.*, 2002; Kayalı *et al.*, 2004).

A free radical can be defined as any neutral, positively or negatively charged species that has one or more unpaired electrons (Halliwell and Gutteridge, 1989). They are produced continuously in cells either as by products of metabolism, or for example, by leakage from mitochondrial respiration, due to the loss of inner mitochondrial membrane permeability barrier. The most important reactions of free radicals in aerobic cells involve molecular oxygen and its derivatives, peroxides and transition metals.

Under normal conditions, lipids are also subject to turnover and damaged lipids can be reprocessed and repaired. However, many of the products of lipid oxidation such as hydroperoxides, alcohols, aldehydes and F2-isoprostanes, have biological activities and can not be repaired (Esterbauer *et al*., 1991; Moore *et al*., 1995). Polyunsaturated fatty acids (PUFA) have a propensity to oxidize rather than saturated fatty acids, resulting in the formation of alkanes, aldehydes, alcohols, and hydroperoxides among other products. The unsaturated bonds of lipids are the main target of free radicals, therefore lipid peroxidation results in the loss of unsaturation (Severcan *et al*., 2005).

1.3.5 Experimental Models of Diabetes Mellitus

There are many advantages to study diabetes mellitus in experimental animals. Almost every diabetic complication can be detected in experimental models of diabetes to investigate the molecular mechanism of the disease. Furthermore, models of experimental diabetes permit the study of the involvement of environmental factors, such as diet, exercise, drugs, toxins and infective agents. In addition they exhibit many features of clinical diabetes. However none of the models is exactly equivalent to clinical diabetes.

The following methodologies have been applied for experimental diabetes:
Surgical Diabetes: This method, which consists of total or subtotal pancreatomy in animals, is now rarely used for investigation of diabetes and its complications.

Spontaneous Diabetes: Diabetes mellitus may occur spontaneously in the population of various animal species like Chinese Hamster and BB Wistar Rat.

Viral Diabetes: Viral infection has been implicated as a cause of diabetes in both man and animals. Several viruses have been reported to induce experimental diabetes in certain animal species: Coxsackie viruses, foot and mouth disease virus, rubella virus, retroviruses etc.

Chemical Diabetes: Various drugs and chemicals have been reported to cause an experimental situation somewhat similar to diabetes. Among these diabetogenic substances alloxan and streptozotocin are the most specific and convenient ones. Among these diabetogenic substances streptozotocin, (2-deoxy-2-(3-methyl-3-nitrosourido) D-glycopyranose) and alloxan (ALL) are widely used inducers of diabetes mellitus in experimental animals, whereas others may exhibit only a weak and reversible diabetogenic activity, and their effects are not specific to the pancreatic β-cells (Lithell and Berne, 1991). Alloxan was the initial agent but has been replaced by STZ as the primary diabetogen for experimental DM. Both agents cause selective destruction of pancreatic β islet cells. Alloxan and STZ are thought to cause DNA strand breaks which activate the repair mechanism/nuclear poly (ADP-ribose) synthetase and deplete the cellular pool of NAD^+, resulting in pancreatic β-cell damage (Gunnarson, *et al.*, 1974). It has been proposed that the basis for the increased pathogenecity of the diabetic state in streptozotocin (STZ)-induced diabetic rats may be due to oxidative stress (Baynes, 1991).

1.3.5.1 STZ Induced Diabetes Mellitus

Streptozotocin is an antibiotic extracted from *Streptomyces achromogenes*. It causes diabetes by a direct action on the pancreatic β-cell. The exact site of STZ interaction with β-cell is somewhat speculative. In previous studies, 7 to 10 h after STZ treatment, massive β-cell degranulation and necrosis associated with an increase in serum insulin levels and hypoglycemia was observed. This was followed by prolonged hyperglycemia (1-28 days), which coincided with a reduction in pancreatic insulin levels <5% of normal values. The diabetogenic effects of STZ were found to be dose dependent, ranging from mild diabetes following a dose 35 mg kg^{-1} to a severe ketotic state, leading to death within 2

to 3 days after a dose of 100 mg kg^{-1}. When treated with intermediate doses of STZ (55-65 mg kg^{-1}), weight loss and blood glucose level 3 to 4 times higher than normal one was seen (Tomlinson *et al*., 1992).

1.4 Effects of Diabetes Mellitus on Skeletal Muscles

Skeletal muscle is one of the major tissues determining carbohydrate and lipid metabolism in the body. Together with liver and brain it is also responsible for glucose disposal, accounting for up to 80% of all glucose uptakes under insulin stimulated conditions; thus it takes role in determination of glucose homeostasis (DeFronzo *et al.*, 1981; Kern *et al.*, 1990; Venojarvi *et al.*, 2005). Similarly, it is the predominant tissue for whole body lipid oxidation, with up to 90% of the energy requirements at rest derived from fatty acids (Kelley *et al.*, 2001; McAninch *et al.*, 2003). Also insulin was found to increase the fatty acid uptake to skeletal muscles (Glatz *et al.*, 2002). Skeletal muscles are the major target of insulin action to regulate blood glucose levels through activation of insulin sensitive glucose transporter, GLUT4, on the plasma membrane (Katz *et al.*, 1996). It is known that in diabetes glucose uptake decreases, as a result glycogen synthesis is impaired (DeFronzo *et al.*, 1987; Golay *et al.*, 1988; Venojarvi *et al*., 2005). Healthy skeletal muscle can utilize either lipid or carbohydrate fuels and can rapidly change its fuel selection upon the stimulus and energy demands (Goodpaster and Wolf, 2004, Goodpaster and Brown, 2005). In diabetes mellitus the loss of flexibility of skeletal muscle to switch between lipid and carbohydrate fuels is observed, and this is an important aspect of insulin resistance in type II diabetes and obesity (Goodpaster and Wolf, 2004).

The muscle to body weight ratios was found to be smaller in diabetic rats (Armstrong and Ianuzzo, 1977). Studies on the ultrastructure of skeletal muscles focused on the thickening of the basement membrane, and changes in mitochondria, myofibril and glycogen content have been observed (Campeanu *et al*., 1971, Chao *et al*., 1976). In many studies an increase in lipid content and triglycerides in diabetes were demonstrated (Lithell *et al.*, 1981, Goodpaster *et.al.*, 1997, Malefant *et al.*, 2001, He *et al.*, 2001; Perseghin *et al.*, 2003).

However, in some studies it was also found that diabetes had no effect on triglyceride or lipid content (Hopp and Palmer, 1991; Bernroider *et al.*, 2006). Stearns *et al.* (1979) demonstrated the increase in fat utilization in skeletal muscles of type I diabetes mellitus rat model. Therefore, there are some contradictory results about the effect of diabetes on lipid composition of the muscle. In different types of skeletal muscles, type I fibers were found to possess an increased content of lipids (He *et al.*, 2004; van Loon *et al.*, 2004).

Many of the chronic complications of diabetes involve changes in structural proteins. Insulin stimulates the uptake of a number of amino acids into the muscle cell, so reduced availability of essential amino acids for protein synthesis may be a factor of diabetic myopathy (Wool *et al.*, 1968; Armstrong and Ianuzzo, 1977). Alterations in protein synthesis and degradation can also adversely affect the repair of the tissue after injury (Charlton and Nair, 1998). There are studies reported an increase in protein breakdown in diabetes, but there are also unexpected findings showing the increase in protein synthesis during insulin deprivation (Bennet *et al.*, 1990; Luzi *et al.*, 1990; Charlton and Nair, 1998). Pacy *et al.* (1991) reported that insulin does not inhibit protein breakdown in diabetic conditions. On the contrary, when data from other studies (Denne *et al.*, 1991; Moller-Loswick *et al*., 1994) are considered, there is little doubt that insulin inhibits protein breakdown. Therefore, there are also controversial results reported in literature.

Previous biochemical and histochemical investigations in STZ-diabetic rats suggest a greater loss in oxidative potential on type II fibers than type I fibers and an altered mitochondrial morphology in both type IIB and type I fibers (Armstrong *et al.*, 1975). Moreover, isolated mitochondria from alloxan-treated rats have been shown to be more fragile than normal (Hall *et al.,* 1960). In type IIB muscles of diabetic animals, the mitochondria cristae were found to be less distinct and fewer in number, and more electron dense granules were observed in mitochondria (Chao *et al.*, 1976). The mitochondria of diabetic type IIA fibers were reduced in number with no apparent morphological changes. In type I fibers of diabetic animals, the mitochondria contained fewer cristea and more granules (Chao *et al.*, 1976).

It has been proposed that type I muscle fibers are not affected strongly from diabetes when the histochemistry of muscles was examined in diabetic conditions (Armstrong *et al*., 1975; Armstrong *et al*., 1977). Later on, other researchers reported that type I muscle fibers have an increased content of insulin-regulated glucose transporters and greater insulin sensitivity for glucose metabolism, therefore; they were reported to be strongly affected from diabetes (He *et al.*, 2001; Kelley and Goodpaster, 2001, Leary *et al.*, 2003).

1.5 Electromagnetic Radiation and Optical Spectroscopy

Electromagnetic radiation is considered as two mutually perpendicular electric and magnetic fields, oscillating in single planes at right angles to each other. These fields are in phase and are propagated as a sine wave as shown in Figure 4, where E is the direction of the electric field while B is the direction of the magnetic field (Stuart, 1997).

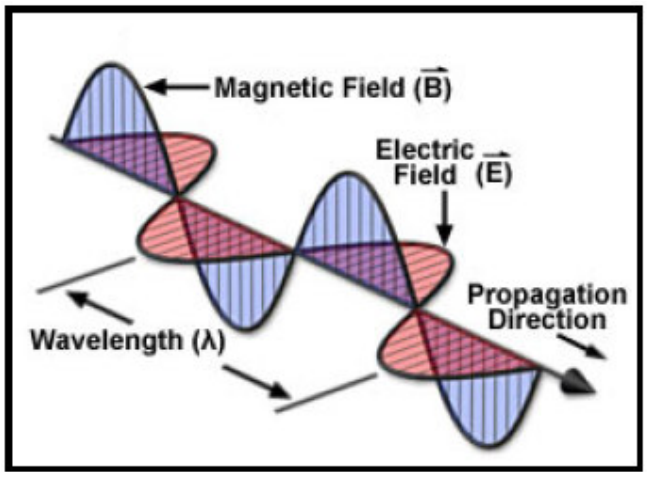

Figure 4. An electromagnetic wave

The energy (*E*) of the electromagnetic wave is given by the Bohr equation as:

$$\Delta E = h\nu$$

ν is the frequency of the applied radiation and h is Planck's constant (h = 6.6×10^{-34} joule second).

$$c = \lambda \nu$$

where c is the speed of light in vacuum (3.0×10^{8} ms^{-1}) and λ is the wavelength of light. These two equations can be used to identify a common spectroscopic

unit called wavenumber, which is denoted by $\bar{\nu}$. Wavenumber is defined as the reciprocal of the wavelength as follows;

$\bar{\nu}$ = wavenumber = $(1/\lambda)$ [has a unit of cm^{-1}]

Thus, $E = h\nu = h c \bar{\nu}$,

From these equations, it is clear that both wavenumber and frequency are directly proportional to energy.

The interaction between electromagnetic radiation and matter can cause redirection of the radiation, it can be scattered (i.e. its direction of propogation changes), absorbed (i.e. its energy is transferred to the molecule) or emitted (energy is released by the molecule). When the energy of the light is absorbed, the molecule is said to be *excited.* An excited molecule can possess any one of a set of discrete amounts (quanta) of energy described by the laws of quantum mechanics. These amounts are called the *energy levels* of the molecule. A typical energy-level diagram describing these energy levels is presented in Figure 5. The thin horizontal lines represent vibrational energy levels. Accordingly, the long arrow exemplifies an electronic transition, while the short arrow typifies a vibrational transition. The lowest electronic level is called the ground state and all others are excited states (Freifelder, 1982).

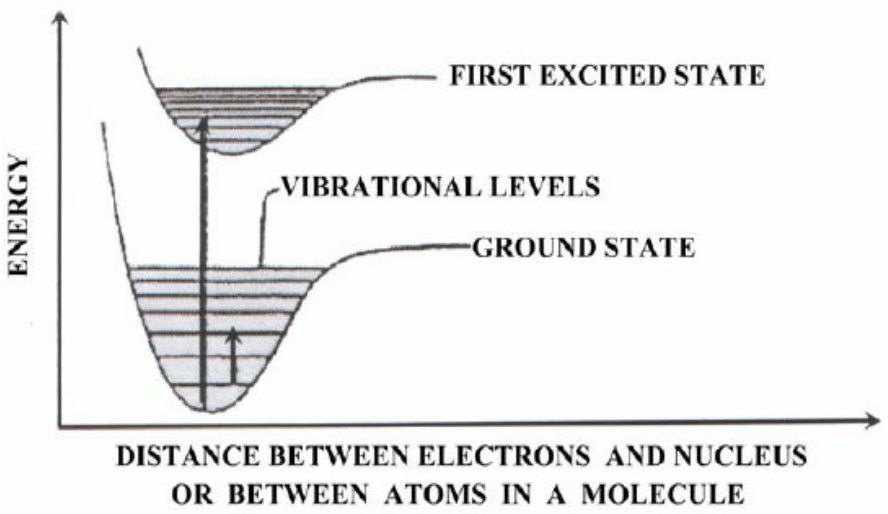

Figure 5. Typical energy-level diagrams showing the ground state and the first excited state. Vibrational levels are shown as thin horizontal lines. A possible electronic transition between the ground state and the fourth vibrational level of the first excited state is indicated by the long arrow. A vibrational transition within the ground state is indicated by the short arrow (Freifelder, 1982).

For most purposes, it is convenient to treat a molecule as if it possesses several distinct reservoirs of energy. The total energy is given by:

$$E_{\text{total}} = E_{\text{transition}} + E_{\text{rotation}} + E_{\text{vibration}} + E_{\text{electronic}} + E_{\text{electron spin orientation}} + E_{\text{nuclear spin orientation}}$$

Each E in the equation represents the appropriate energy as indicated by its subscript. In solution, a molecule can translate, rotate and vibrate. The energies associated with each of these are quantized (Campbell, 1984). The contributions of $E_{\text{translation}}$, $E_{\text{electron spin orientation}}$ and $E_{\text{nuclear spin orientation}}$ are negligible because the separations between respective energy levels are very small. The separations between the neighboring energy levels corresponding to E_{rotation}, $E_{\text{vibration}}$ and $E_{\text{electronic}}$ are associated with the microwave, infrared and ultraviolet-visible region of the electromagnetic spectrum, respectively (Campbell and Dwek, 1984). The means of study for these energy transitions is standard absorption spectroscopy for electronic transition, infrared and Raman spectroscopy for vibrational and rotational transitions and nuclear magnetic resonance for nuclear spin orientation (Freifelder, 1982).

Spectroscopy is defined as the study of the interaction of electromagnetic radiation with matter. Spectroscopic techniques involve irradiation of a sample with some form of electromagnetic radiation, measurement of the scattering, absorption, or emission in terms of some measured parameters, and the interpretation of these measured parameters to give useful information. Figure 6 represents many of the important regions of the electromagnetic spectrum.

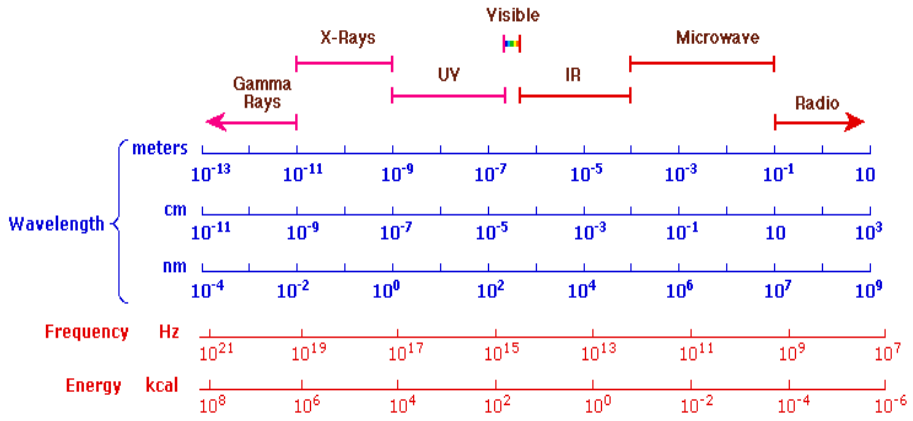

Figure 6. The Electromagnetic spectrum

1.5.1 Basis of Infrared Spectroscopy

The term "infrared" covers the range of the electromagnetic spectrum between 0.78 and 1000 μm. In the context of infrared spy, wavelength is measured in "wavenumber".

Infrared (IR) region is divided into three sub regions (Smith, 1999):

Region	Wavenumber range (cm^{-1})
Near	14000-4000
Middle	4000-400
Far	400-4

Infrared spectroscopy has been used in a number of branches of science as a quantitative and qualitative tool (Diem, 1993). The energy of most vibrational transitions corresponds to the infrared region of the electromagnetic spectrum. Hence, the interaction of infrared radiation with matter is associated with molecular vibrations. Bond lengths and bond angles are continuously changing

due to this vibration. A molecule absorbs infrared radiation when the vibration of the atoms in the molecule produces an oscillating electric field with the same frequency as the frequency of the incident IR light. The molecule will only absorb radiation if the vibration is accompanied by a change in the dipole moment of the molecule. A dipole occurs when there is charge separation across bond. If the two oppositely charged molecules get closer or move further apart as the bond bends or stretches, the moment will change. All of the motions can be described in terms of two types of molecular vibrations. One type of vibration, a stretch, produces a change of bond length. A stretch is a rhythmic movement along the line between the atoms so that the interatomic distance is either increasing or decreasing. A stretch can be symmetric or asymmetric. The second type of vibration, a bend, results in a change in bond angle. Bending can occur in the plane of the molecule or out of plane; it can be scissoring, like blades of a pair of scissors, or rocking, where two atoms move in the same directions (Arrondo *et al.*, 1993). Consequently, infrared spectra are generated by the characteristic motions of various functional groups (e.g. methyl, carbonyl, amide etc.). The sensitivity of these modes of vibration to any alteration in chemical structure, conformation, and environment presents the value of infrared spectroscopy. Figure 7 demonstrates the main types of variations schematically.

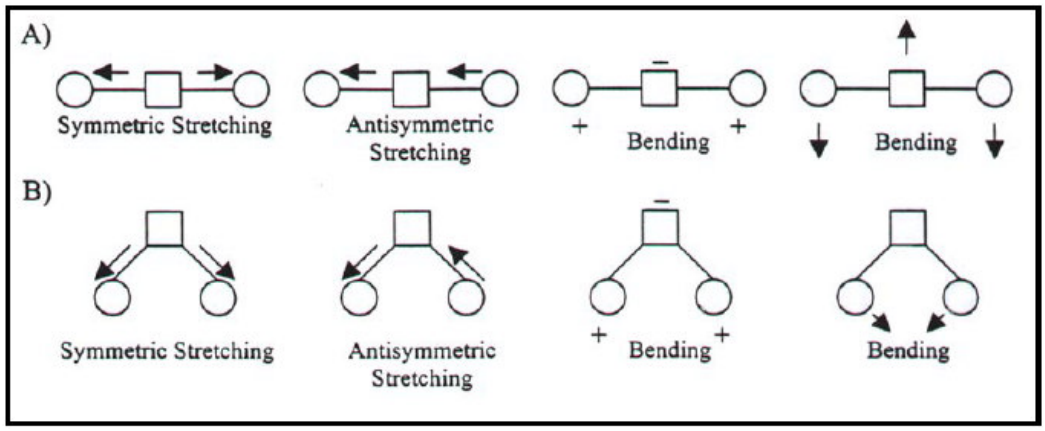

Figure 7. The schematic representation of some molecular vibrations in linear triatomic molecules (A) and non-linear triatomic molecules (B). (+) and (-) symbols represent atomic displacement out of page plane (Arrondo *et al.*, 1993).

Upon interaction with infrared radiation, portions of the incident radiation are absorbed at particular wavelengths. The multiplicity of vibrations occurring simultaneously produces a highly complex absorption spectrum, which is the plot of absorption as a function of wavenumber (ν) expressed in terms of cm^{-1}. The value of infrared spectral analysis comes from the fact that the modes of vibration of each group are very sensitive to the changes in chemical structure, conformation and environment. In addition, as each different material has a unique combination of atoms, no two compounds produce the exact same infrared spectrum. Therefore, an infrared spectrum can result in a positive identification of every different kind of material.

1.5.2 Fourier Transform Infrared Spectroscopy (FTIR)

Fourier transform infrared (FTIR) spectroscopy has found increasing favor in laboratories since early eighties. The basic components of a Fourier transform infrared spectroscopy (FTIR) are visualized in Figure 8.

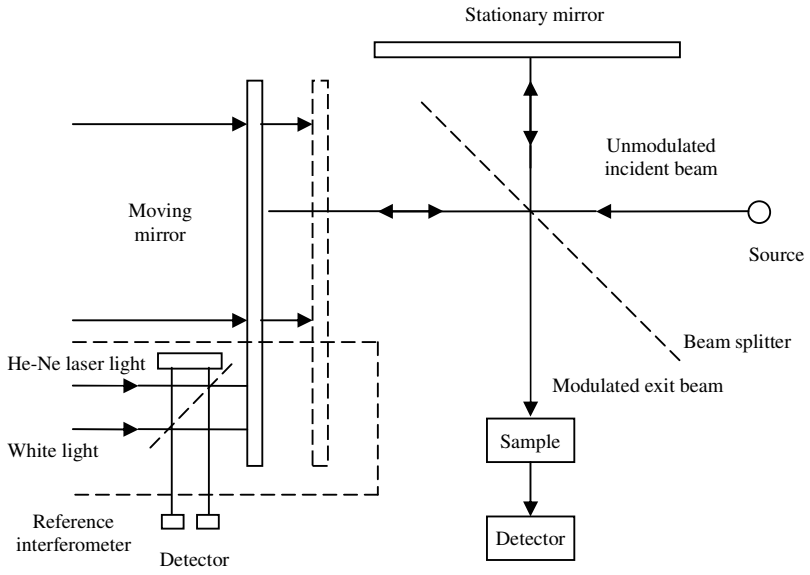

Figure 8. The basic components of FTIR spectroscopy.

This method is based on the idea of the interference of radiation between two beams to yield an *interferogram,* which is a signal produced as a function of the change of pathlength at a beam splitter. The most important feature of an

interferogram is that every individual data point of this signal contains information over the entire infrared region. This process is carried by an interferometer. It encodes the initial frequencies into a special form, which the detector can observe. For rapid-scanning interferometers liquid nitrogen cooled *mercury cadmium telluride (MCT)* detectors are used. For slower scanning types of interferometer, pyroelectric detectors (e.g. a *deuterated triglycine sulfate (DTGS)* detector element) can be used. In essence, the detector is always observing all frequencies at the same time (Griffiths and De Haseth, 1986). The two domains of distance and frequency are interconvertible by the mathematical method of Fourier transformation. Therefore, Fourier transformation is simply a mathematical means of sorting out the individual frequencies for the final representation of an infrared spectrum.

1.5.3 The Advantages of FTIR Spectroscopy

The reason why infrared spectroscopy is commonly used is that
- Sample preparation is very easy,
- Samples can be prepared in gaseous, liquid, or solid states,
- Qualitative interpretation is possible,
- Rapid data acquisition is possible, especially with Fourier transform infrared spectroscopy, and
- The price is considerably more reasonable, especially compared to NMR spectroscopy (Diem, 1993).

Moreover, due to its somewhat different technology, it is used to examine functional groups that are not accessible with ultraviolet and visible light absorption spectrometers (Freifelder, 1982).

The main advantage of FTIR spectroscopy lies in its ability to increase signal-to-noise ratio by signal averaging (Stuart, 1997).
- For biological studies is that spectra of almost any biological material can be obtained in a wide variety of environments.
- It provides a precise measurement method, which requires no external calibration.

- It is possible to examine all wavelengths arriving at the detector simultaneously, compared to being able to sample only one spectral element at a time by the detector (Diem, 1993).
- This method is a rapid and sensitive technique, which is easy to perform to improve the signal-to-noise ratio (noise adds up as the square root of the number of scans, whereas signal adds linearly). The data processing is simple with the computer softwares. Moreover, system permits permanent data storage, manipulation of data and quantitative calculations ((Rigas *et al.*, 1990; Manoharan *et al.*, 1993; Yono *et al.*, 1996; Ci *et al.*, 1999).
- The instrumentation is inexpensive compared to the cost of X-Ray diffraction, NMR, ESR, and CD spectroscopic equipment.
- Small sample quantities are sufficient to analyse and in vivo studies are possible (Mendelsohn and Mantsch, 1986).
- It is a non-destructive technique (Melin *et al.*, 2000, Severcan and Haris, 1999, Çakmak *et al.*, 2003) and there is no light scattering or fluorescent effects.
- The system can be applied to the analysis of any kind of material and that is not limited to the physical state of the sample. Samples may be solutions, viscous liquids, suspensions, inhomogeneous solids or powders (Colthup *et al.*, 1975). Indeed, kinetic and time-resolved studies are possible (Mantsch *et al*., 1984; Mendelson and Mantsch, 1986 and Haris and Severcan, 1999).
- Frequency and bandwidth values can be determined routinely with uncertainties of better than ±0.05 cm^{-1}.

1.5.4 Applications of Fourier Transform Infrared Spectroscopy

One of the useful aspects of FTIR spectroscopy is the fact that any group or bond in a molecule gives rise to characteristic band(s) in the infrared spectra. Thus, these characteristic spectral features can simply be assigned to the particular groups or bonds in the corresponding molecules. This approach in vibrational spectroscopy is referred to as group frequencies (Diem, 1993). Hence; spectra can be examined in several groups depending on the type group frequency.

Generally, there are few infrared bands in the 4000-1800 cm^{-1} wavenumber range and many bands in the 1800-400 cm^{-1} range (Stuart, 1997). The information available from an FTIR spectrum are reflected from the form of band shapes, peak heights, half widths, frequency shifts and integrated intensity of the vibrational bands (Lamba *et al.*, 1991).

The bands in the 3050-2800 cm^{-1} spectral region are generally termed as the carbon-hydrogen (C-H) stretching vibrations and they correspond to the acyl chain modes. The vibrational modes in this region can be used as sensitive monitors of the state-of-order of the membrane lipid matrix (Casal and Mantsch, 1984; Severcan, 1997). The CH_2 symmetric stretching vibration band is particularly valuable for the monitoring of the state-of-order of biological membranes because its' frequency and bandwidth parameters respond sensitively to changes in the order and mobility of fatty acid chains, respectively; and since the contributions from other vibrational modes is minimal (Mantsch, 1984; Schultz and Naumann, 1991). A shift in the frequency to higher values indicates a diminished state-of-order of the cellular membrane system suggesting an increase in the number of gauche conformers (Casal and Mantsch, 1984; Mantsch, 1984; Severcan *et al*, 1995). On the other hand, an increase in the bandwidth is associated with a greater motional freedom (Boyar and Severcan, 1997; Mantsch, 1984). Moreover, it seems reasonable that when the protein composition of a membranous system is altered, this in turn can have an effect on the membrane state-of-order via lipid-protein interactions. For example; an increase in the relative protein content would cause a reduction in the state-of-order of the membrane structure (Kneipp *et al*, 2000).

The bands in the 1800-400 cm^{-1} region, which is generally called the fingerprint region, originate both from the vibrations of the interfacial and head-group modes of the membrane lipids. However, this region also corresponds to the protein and nucleic acid vibrational modes (Mendelsohn and Mantsch, 1986). Lipids can exist in one or more of numerous polymorphic forms between which they can interconvert depending on the conditions in the medium. These alterations are usually called phase transitions. However, lipid

structures are generally existent in two physical states, the ordered, rigid gel phase and the more fluid, disordered liquid crystalline phase. The thermally induced transition between these two phases, which is generally called the gel-to-liquid crystal phase transition, produces considerable changes in the infrared spectrum. FTIR spectroscopy has proven to be a very useful and effective tool in the detection, assignment, and characterization of these lipid phase transitions. The important course of action during the interpretation of the phase transitions is to correlate the changes in the spectroscopic parameters induced by the lipid phase transition with the changes that are known to occur in the structure of the lipids during those processes (Mendelsohn and Mantsch, 1986).

During the last years, the use of FTIR to determine the structure of proteins has dramatically expanded. The complete three-dimensional structure of a protein at high resolution can be determined by X-ray crystallography and nuclear magnetic resonance (NMR) spectroscopy, which are the most powerful techniques available by far. However, both techniques has considerable disadvantages: X-ray crystallography requires high-quality single crystals which are not available for many proteins and the structure of a protein in crystal may not always relate to its structure in solution; NMR spectroscopy can determine the structure of proteins in solution, but the interpretation of the NMR spectra of large proteins is complex, and the technique is presently limited to small proteins (~30 kDa) (Haris and Severcan, 1999). These limitations have led to the development of alternative methods, such as FTIR, that are not able to generate structures at atomic resolution but provide also structural information on proteins (especially on secondary structure).

The most important advantage of FTIR spectroscopy for structural characterization of proteins is that spectra of almost any protein can be obtained in a wide variety of environments. Spectra of a protein can be obtained in single crystals, aqueous solution, detergent micelles, lipid membranes, etc. Moreover, FTIR requires only small amounts of protein (10 μg), and the size of the protein is not important (Haris and Severcan, 1999). With developments in FTIR instrumentation it is now possible to obtain high

quality spectra from dilute protein solutions in H_2O (Haris and Chapman, 1992; Arrondo and Goñi, 1999). The overlapping H_2O absorption bands can be digitally subtracted from the spectrum of the protein solution. In addition, the broad infrared bands in the spectra of the proteins can be analyzed in detail by using second derivative and deconvolution procedures. These procedures can be utilized to reveal the overlapping components within the broad absorption bands (Haris and Chapman, 1992; Arrondo and Goñi, 1999). The FTIR spectrum of a protein is characterized by a set of absorption regions known as amide modes. From these modes, Amide I that is located between 1700 and 1600 cm^{-1} and composed mainly (~80 %) by the C=O stretching vibration of the peptid bond, can be analyzed for structural characterization of proteins. This band can be decomposed into its constituents by curve-fitting procedures and compared with a set of spectra of proteins with known structure (Arrondo and Goñi, 1999). By this way, secondary structure of proteins can be studied by FTIR.

1.6 Aim of the Study

Skeletal muscle is one of the major tissues determining carbohydrate and lipid metabolism in the body and is the major target of insulin action; therefore, skeletal muscle is affected from diabetes. The effects of diabetes on skeletal muscle tissues gained attention in the early 1960s and ultrastructural changes occurring in skeletal muscles in diabetes have been clearly demonstrated by the histochemical analysis. Although numerous studies have been carried out concerning this topic, most of them are clinical reports that used human subjects. In clinical studies, the administration of insulin to subjects treats the effects of diabetes to some extent, and the sole effect of diabetes can not be seen.

Moreover, the studies concerning the effect of diabetes on skeletal muscle tissues revealed controversial results on protein and lipid content, and their breakdown or synthesis metabolisms. Although the mechanism of type I diabetes is known, its effects on structure and function of the whole macromolecular composition of skeletal muscle tissue remain unclear yet.

Therefore, this current study is conducted to determine the effects of type I diabetes on the whole macromolecular composition of two types of skeletal muscles, namely Soleus (SOL) and Extensor Digitorum Longus (EDL). For this purpose FTIR spectroscopy was employed.

FTIR spectroscopy is a valuable technique due to its high sensitivity in detecting changes in the functional groups belonging to tissue components at the same time. The technique is especially useful for the analysis of secondary structural characterization of proteins. This technique is non-destructive, and highly selective because its ability to be a spectral fingerprint for molecular components.

The other aim of this study is to apply FTIR spectroscopy as a rapid and suitable method to evaluate the effect of diabetes on skeletal muscle tissues at molecular level and to compare these findings with biochemical and physiological data obtained in other studies.

CHARTER 2

MATERIALS AND METHODS

2.1 Materials

Streptozotocin (STZ) was purchased from Sigma (Sigma Chemical Company, Saint Louis, Missouri, USA) and potassium bromide (KBr) was obtained from Merck (Merck Company, Darmstadt, Germany). All chemicals were obtained from commercial sources at the highest grade of purity available.

2.2 Preparation of Experimental Animals

Adult male Wistar rats (12-14 weeks) weighing 250-300g which are obtained from Experimental Animal Center, Adnan Menderes University, Aydin, were selected randomly. The rats were fed with a Standard diet with water ad libitum, and kept in conventional room with controlled light (12:12, dark:light), temperature (22±1 °C), relative humidity (40-50%) and ventilation (15 air changes per hour). They were allowed to adapt to their environment for 1 week prior to the experiments. All procedures used in the experiments were approved by the Ethics Committee of Adnan Menderes University.

The rats were separated into two groups as control (n=7) and diabetic (n=7). Control rats received citrate buffer (0.05 mol/L, pH 4.5) injection as a single dose, intraperitoneally. Diabetes induction was made by a single intraperitoneal dose of streptozotocin (STZ) (50 mg/kg) dissolved in 0.05 M citrate buffer (pH 4.5). The rats were given 5% dextrose solution to prevent the deaths due to hypoglycemic shock that can take place in the first 6 hours after STZ administration.

Blood glucose levels were measured 3 days after the STZ administration using a glucometer (One Touch Horizon Blood Glucose Monitoring System/Glucometer, USA). Rats with blood glucose levels higher than 300 mg/dl were accepted as diabetic. At the end of the 6th week, the rats were decapitated, their Soleus (SOL) and Extensor Digitorum Longus (EDL) muscles were dissected separately and stored at -80 ˚C until use. In Figure 9 muscles of pelvic limb of rat are shown, and the places of SOL muscle and tendon of EDL muscle can be seen from this figure.

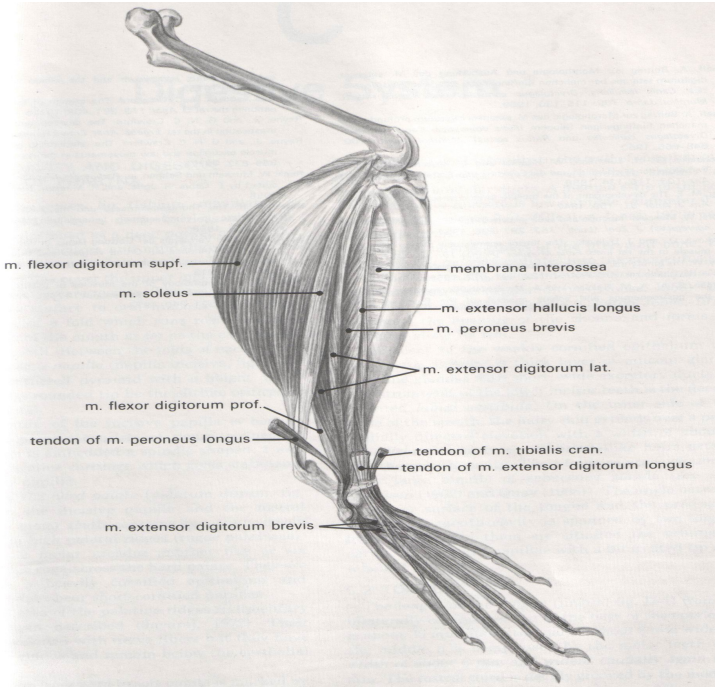

Figure 9. Rat muscles of pelvic limb, lateral aspect (Hebel and Stromberg, 1976).

2.3. FTIR Spectroscopic Measurements

2.3.1 Sample Preparation for FT-IR Studies

The muscle fiber samples were dried in a LABCONCO freeze drier (Labconco FreeZone®, 6 liter Benchtop Freeze Dry System Model 77520) overnight in order to remove the water content. The samples then were ground in a liquid nitrogen-cooled colloid mill (Retsch MM200) to obtain tissue powder. The tissue powder was mixed with dried potassium bromide at the ratio of 0.5 mg sample to 150 mg KBr in a mortar. KBr is most commonly used alkali halide

disk serving as a beam condensing system. It is completely transparent in the mid-infrared region (Stuart, 1997). The mixture was dried again in the freeze drier for 18 hours to remove all traces of remaining water. In this procedure the water solution of sample and halide is frozen and a strong vacuum is applied to frozen solid. The mixture then was compressed into a thin KBr disk under a pressure of ~100kg/cm^2 (1300psi) for 6 min. in an evacuated die. This sinters the mixture and produces a clear transparent disk (Stuart, 1997).

2.3.2 FTIR spectroscopy

Infrared spectra were obtained using a Perkin-Elmer SpectrumOne FTIR spectrometer (Perkin-Elmer Inc., Norwalk, CT, USA) equipped with a MIR TGS detector. Water and carbondioxide molecules in the air affect the IR spectrum. Moreover, although the used KBr is always infrared spectroscopic grade, there is a possibility that it may give some small absorbtion bands interfering with sample spectra. To overcome these problems the spectrum of air and KBr transparent disk was recorded together as background and substracted automatically by using appropriate software (SpectrumOne software).

The spectra of muscle samples were recorded in the 4000-400 cm^{-1} region at room temperature. Each interferogram was collected with 50 scans at 4 cm^{-1} resolution. Each sample was scanned under the same conditions with three different pellets, all of which gave identical spectra. The average spectra of these three replicates were used in detailed data analysis and statistical analysis. Collections of spectra and data manipulations were carried out using SpectrumOne software (Perkin-Elmer). The band positions were measured using the frequency corresponding to the center of weight. Using the same software, the spectra were first smoothed with nineteen-point Savitsky-Golay smooth function to remove the noise. After the averages of three replicates of the same samples were taken, the spectra were baseline corrected. The spectra were normalized with respect to specific bands for visual demonstration. The purpose of the normalization is to remove differences in peak heights between the spectra acquired under different conditions. It allows a point-to-point

comparison to be made (Smith, 1999). The ratios of the intensities and shifting of the frequencies were examined before the normalization process. Band areas were calculated from smoothed and baseline corrected spectra using SpectrumOne software. The bandwidth values of specific bands were calculated as the width at 0.75x height of the signal in terms of cm^{-1}.

For cluster analysis, second derivatives of the spectra were calculated and subsequently vector normalized over the investigated frequency range. Hierarchical cluster analysis was performed on first derivative spectra using the cluster analysis module of OPUS 5.5 (Bruker Optic, GmbH). It was applied to distinguish between different spectra from control and diabetic groups of each muscle types, and control groups of EDL and SOL muscles using a frequency range between 4000-400 cm^{-1}. As input data for cluster analysis, spectral distances were calculated between pairs of spectra as Pearson's correlation coefficients (Helm *et al*. 1991). Cluster analyses for separation of control and diabetic tissue was based on the Euclidean distances. In all cases, Ward's algorithm was used for hierarchical clustering. The samples that can not be discriminated from other groups were labeled with * and were not involved in statistical calculations.

2.4 Statistical Test

The results were expressed as 'mean ± standard deviation (SD)'. Control and diabetic data were analyzed statistically using non-parametric Mann–Whitney U test with the Minitab statistical Software Release 13.0 program. A 'p' value less than or equal to 0.05 was considered as statistically significant. The degree of significanca was denoted as less than or equal to $p<0.05$*, $p<0.01$**, $p<0.001$***.

CHAPTER 3

RESULTS

3.1 General FTIR Spectrum and Band Assignment of Skeletal Muscle Tissue

This work is precisely adressed to investigate the effects of Type I Diabetes Mellitus on the structure of two types of skeletal muscle tissues, namely Soleus (SOL) and Extensor Digitorum Longus (EDL), by using FTIR spectroscopy. SOL muscle is largely composed of type I fibers, whereas EDL is largely composed of type II fibers (Ariano *et al.*, 1973; Delp *et al.*, 1996).

Since the positions and intensities of many of the infrared absorption bands can be correlated with the presence of specific groups of atoms in the system studied (Steele, 1971), it is possible to assign specific wavelength molecular absorption bands to specific vibrational modes of particular functional groups. In this study the same approach was applied.

Figure 10 demonstrates the representative infrared spectrum of control EDL and SOL muscles in 4000-400 cm^{-1} region. The main bands are labelled in this Figure and detailed band assignments are based upon this work and other studies cited in literature (Rigas *et al.*, 1990; Wong *et al.*, 1991; Takahashi *et al.*, 1991; Wang *et al.*, 1997; Jamin *et al.*, 1998; Melin *et al.*, 2000; Jackson *et al.*, 1998;; Lyman *et al.*, 1999; Chiriboga *et al.*, 2000; Çakmak *et al.*, 2003, Banyay *et al.*, 2003; Toyran *et al.,* 2006, Cakmak *et al.*, 2006) were given in Table 1.

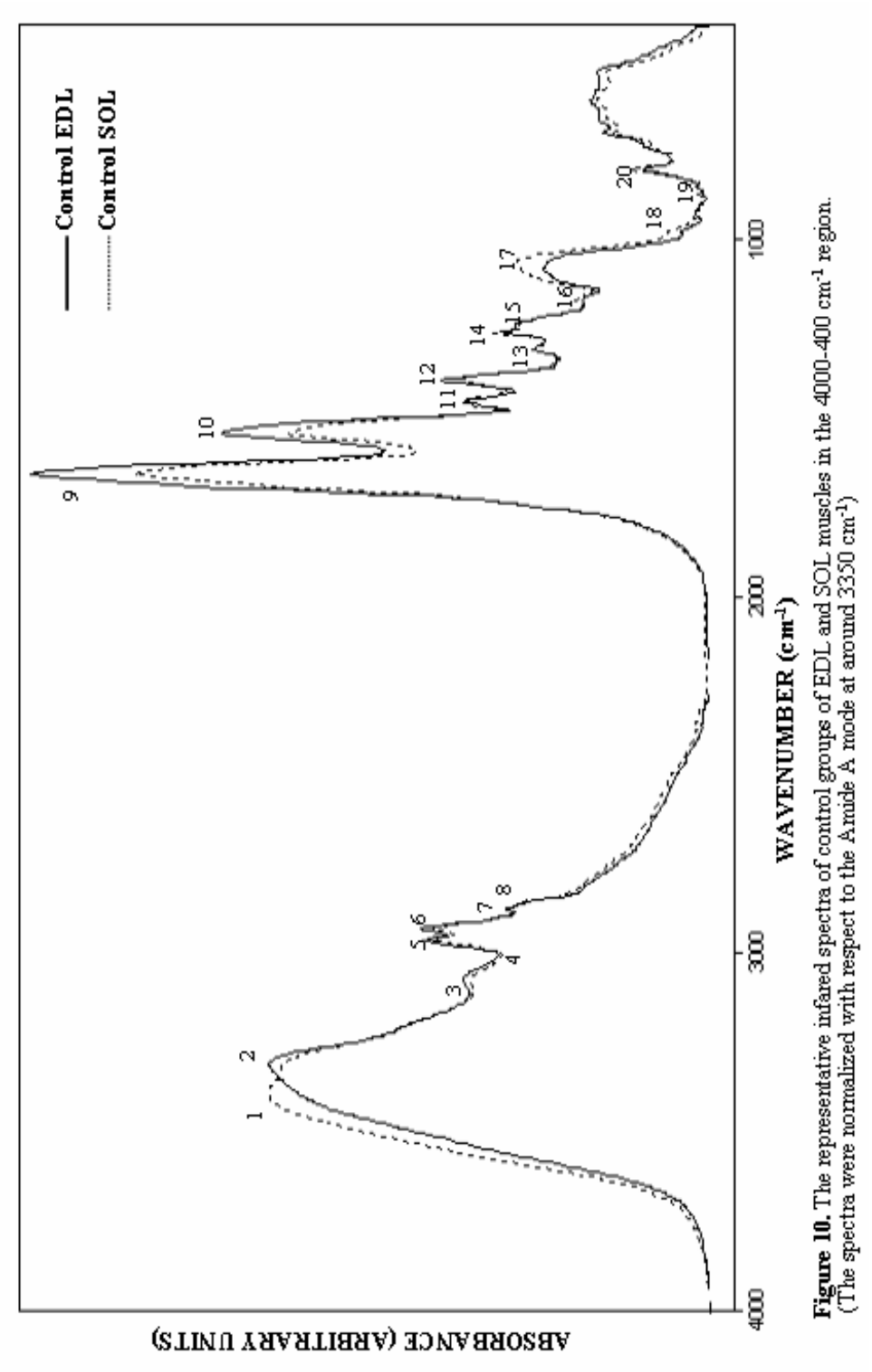

Figure 10. The representative infared spectra of control groups of EDL and SOL muscles in the 4000-400 cm^{-1} region. (The spectra were normalized with respect to the Amide A mode at around 3350 cm^{-1})

As seen from the Figure there are marked differences in the intensity and frequency values of the control groups of EDL and SOL muscles. On the basis of these spectral differences, cluster analysis was performed to differentiate between the control groups of EDL and SOL muscles with a high accuracy (success rate 6/7 tissues for SOL, and 7/7 tissues for EDL). The result is demonstrated in Figure 11.

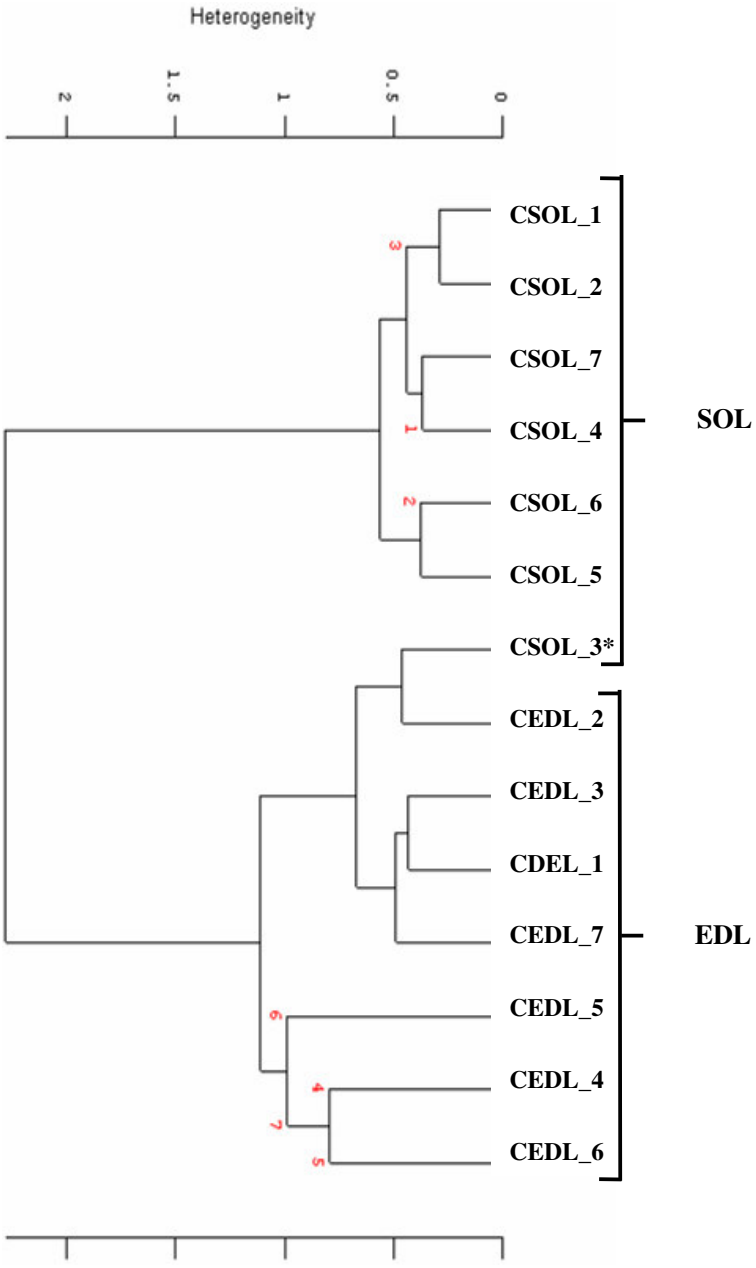

Figure 11. Hierarchial clustering of control groups of EDL and SOL muscles using second derivative spectra (spectral range: 4000-400 cm^{-1}). The sample labelled with * was not clearly differentiated, and not used in statistical analysis.

Table 1. General band assignment of skeletal muscle

Peak numbers	Wavenumbers (cm^{-1})	Definition of the spectral assignment
1	3400	O-H stretching (Amide A), hydrogen-bonded intermolecular OH groups of proteins and glycogen
2	3307	Mainly N-H stretching (Amide A) of proteins with the little contribution from O-H stretching of polysaccharides and intermolecular H bonding
3	3068	C-H and N-H stretching (Amide B) of protein
4	3014	Olefinic=CH stretching vibration: unsaturated lipids, cholesterol esters
5	2962	CH_3 asymmetric stretch: mainly lipids, with the little contribution from proteins, carbohydrates, nucleic acids
6	2929	CH_2 asymmetric stretch: mainly lipids, with the little contribution from proteins, carbohydrates, nucleic acids
7	2874	CH_3 symmetric stretch: mainly proteins, with the little contribution from lipids, carbohydrates, nucleic acids
8	2855	CH_2 symmetric stretch: mainly lipids, with the little contribution from proteins, carbohydrates, nucleic acids
9	1656	Amide I (protein C=O stretching)
10	1540	Amide II (protein N-H bend, C-N stretch)
11	1452	CH_2 Bending: mainly lipids, with the little contribution from proteins
12	1392	COO^- symmetric stretch: fatty acids
13	1343	Amide III vibrations of collagen
14	1261	PO^-_2 asymmetric stretch, non-hydrogen-bonded: mainly nucleic acids with the little contribution from phospholipids
15	1236	PO^-_2 asymmetric stretch, fully hydrogen-bonded: mainly nucleic acids with the little contribution from phospholipids
16	1170	CO-O-C asymmetric stretching: glycogen and nucleic acids
17	1080	PO^-_2 symmetric stretching: nucleic acids and phospholipids C-O stretch: glycogen, polysaccharides, glycolipids
18	976	$C\text{-}N^+\text{-}C$ stretch: nucleic acids, ribose-phosphate main chain vibrations of RNA
19	873	Vibrations in N-type sugars in nucleic acid backbone
20	802	Vibrations in N-type sugars in nucleic acid backbone

3.2 Comparison of Spectra of Skeletal Muscle Fiber Types

3.2.1 Comparison of Control and Diabetic SOL Skeletal Muscle Fiber

FTIR spectral data were collected over the frequency range of 4000-400 cm^{-1}. In order to display the details of spectral changes, the analysis was performed in two distinct frequency ranges. The first range was between 3600-2800 cm^{-1} and the second was between 2000-400 cm^{-1}. All control spectra are overlapped. All diabetic spectra which are different than control spectra, are also overlapped. For this reason, for the following discussions only one control and diabetic spectra will be chosen as a representative spectrum.

Figure 12 shows the infrared spectra of control and diabetic SOL muscle in 3650-3000 cm^{-1} region. Figure 13 shows the infrared spectra of control and diabetic SOL muscle in 3025-2800 cm^{-1} region. As it could be seen from this figure control and diabetic spectra considerably differ in peak positions, peak heights and widths in this region.

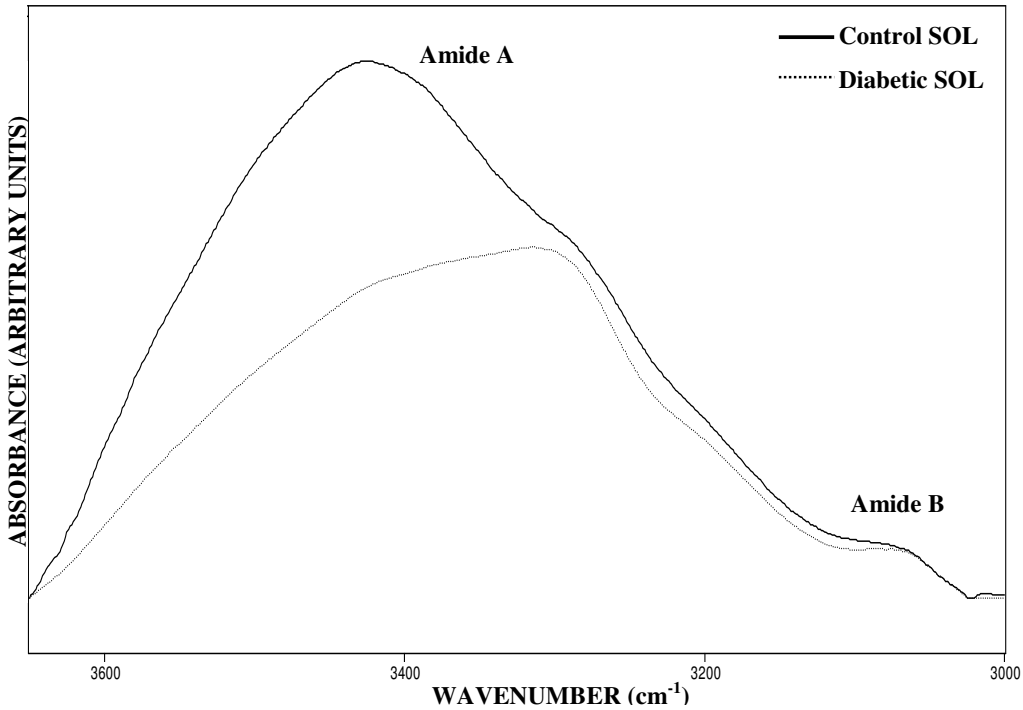

Figure 12. The representative infrared spectra of control and diabetic SOL muscles in the 3650-3000 cm^{-1} region. (The spectra were normalized with respect to the CH_2 asymmetric stretching mode at 2925 cm^{-1})

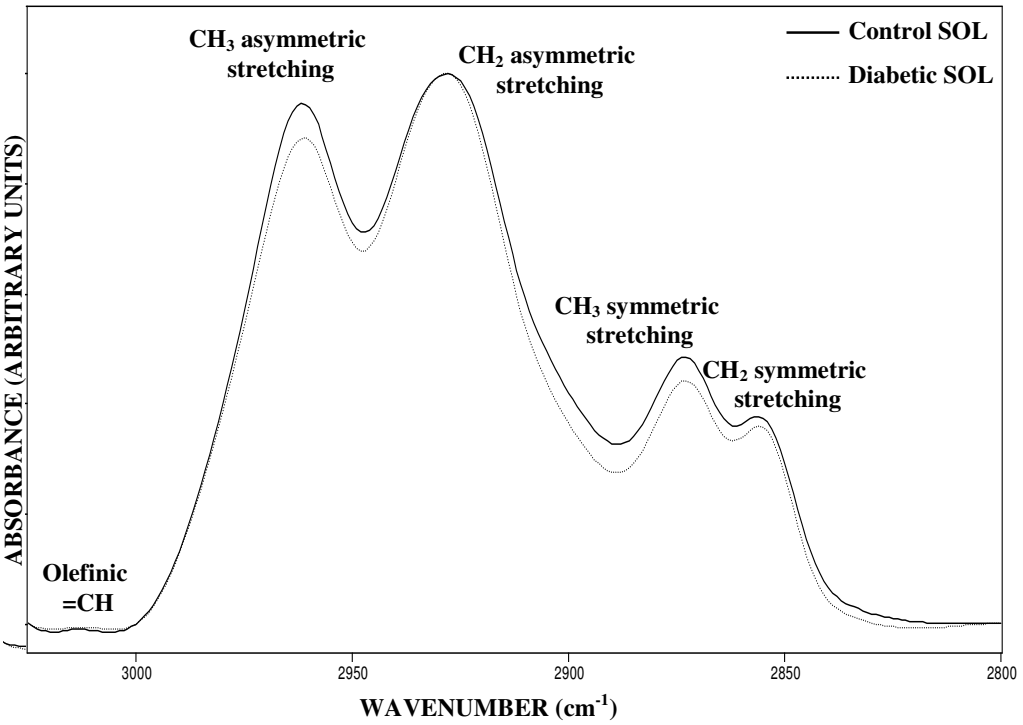

Figure 13. The representative infrared spectra of control and diabetic SOL muscles in the 3025-2800 cm^{-1} region. (The spectra were normalized with respect to the CH_2 asymmetric stretching mode at 2925 cm^{-1})

Figure 14 demonstrates the infrared spectra of control and diabetic SOL muscle in 2000-400 cm^{-1} region. As it could be seen from the Figure, the control and diabetic spectra exhibit remarkable differences in bandwidth, intensity and frequency values in this region. These differences between the control and diabetic spectra will be later discussed more specifically.

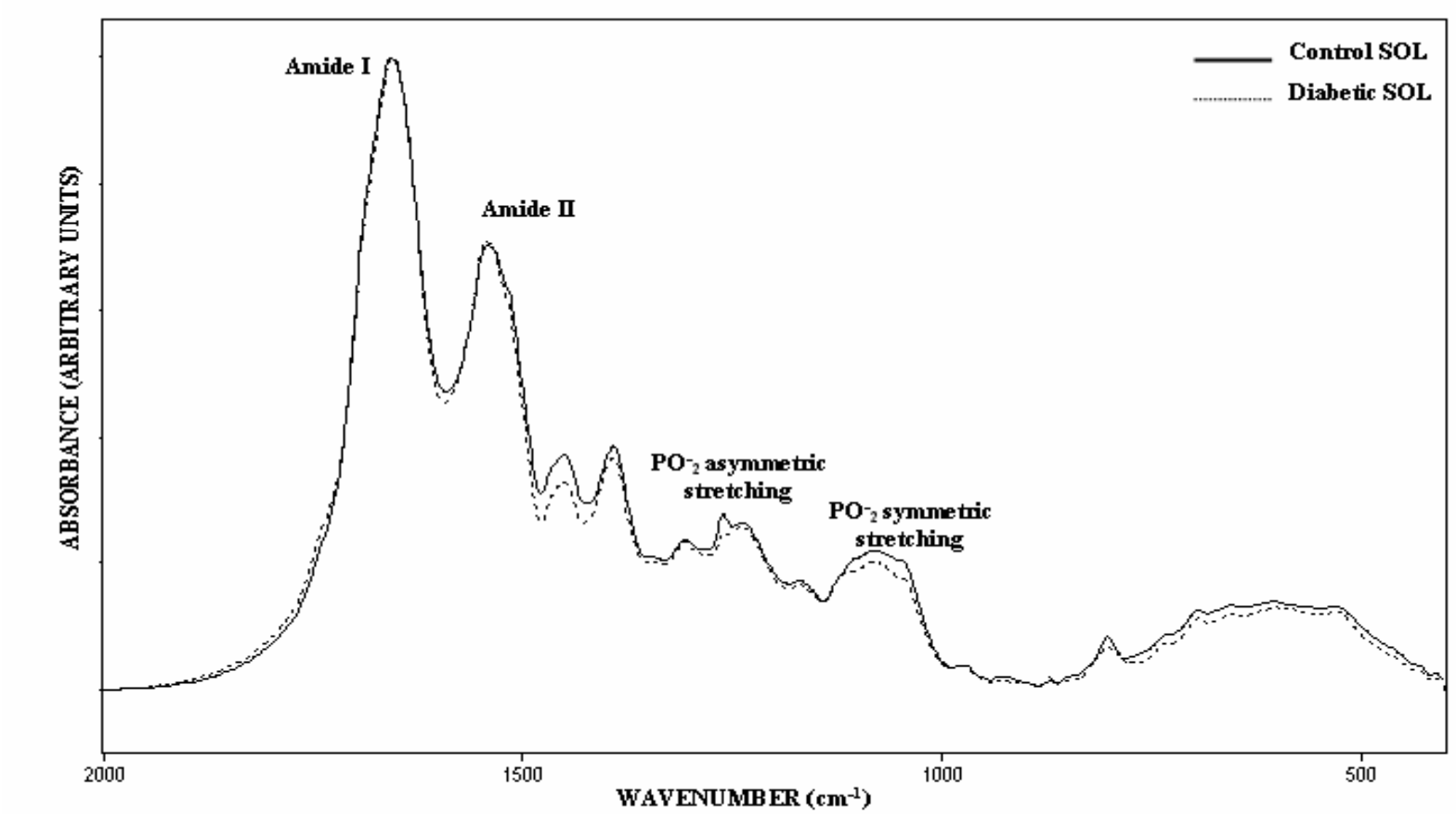

Figure 14. The representative infared spectra of control and diabetic SOL in the 2000-400 cm^{-1} region. (The spectra were normalized with respect to the Amide I at 1645 cm^{-1})

Regarding these spectral differences, the control and diabetic SOL muscles were differentiated using cluster analysis with a high accuracy (success rate 6/7 tissues). The result is demonstrated in Figure 15.

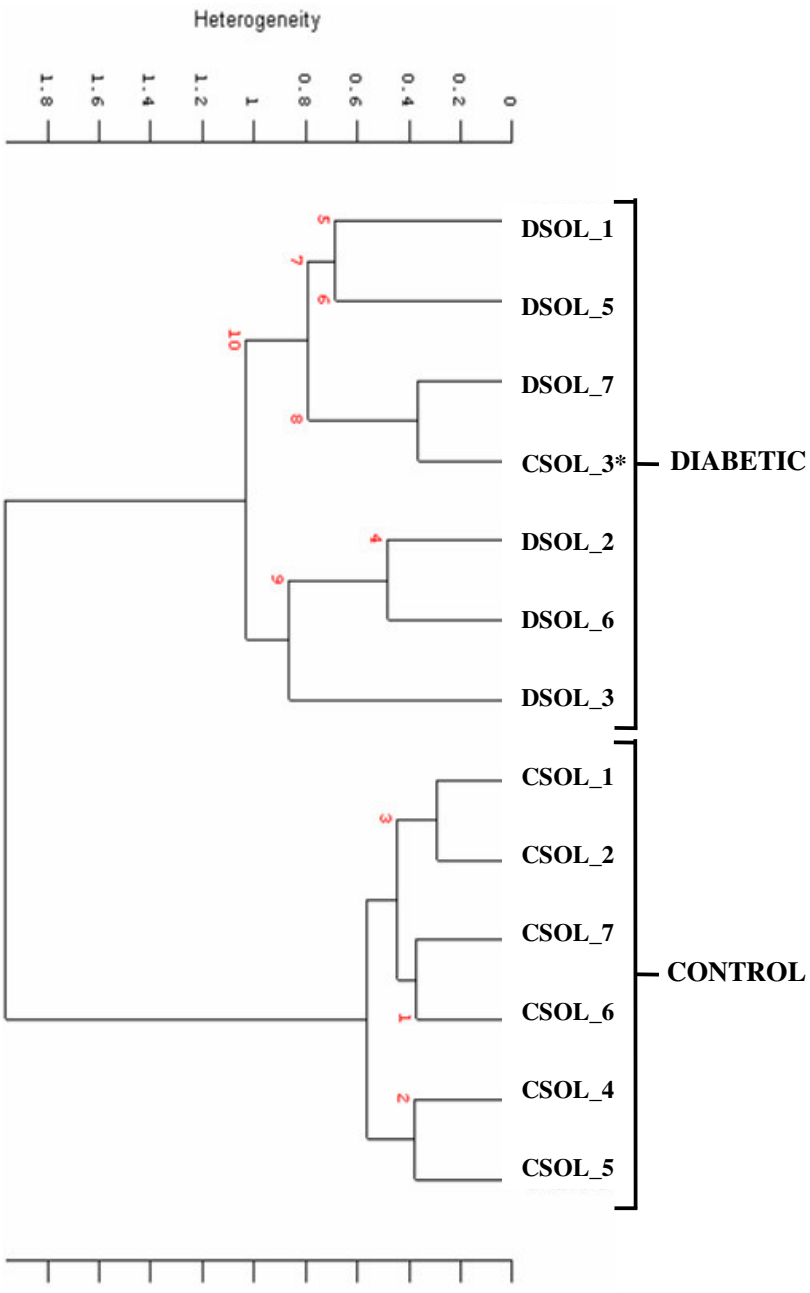

Figure 15. Hierarchial clustering of control and diabetic SOL muscles using second derivative spectra (spectral range: 4000-400 cm^{-1}). The sample labelled with * was not clearly differentiated, and not used in statistical analysis.

3.2.2 Comparison of Control and Diabetic EDL Skeletal Muscle

Figure 16, Figure 17 and Figure 18 shows the infrared spectra of control and diabetic EDL muscle in 3650-3000 cm^{-1}, 3025-2800 cm^{-1} and 2000-400 cm^{-1} regions, respectively. As it could be seen from these Figures control and diabetic spectra considerably differ in peak positions, peak heights and widths in both of the regions. These differences between the control and diabetic spectra will be later discussed more specifically. The differences in variables are similar to main ones observed in part 3.2.1, the spectra of SOL muscle.

To clearly observe these spectral differences, cluster analysis was performed to differentiate between the control and diabetic EDL muscles with a high accuracy (success rate 6/7 tissues). The result is demonstrated in Figure 19.

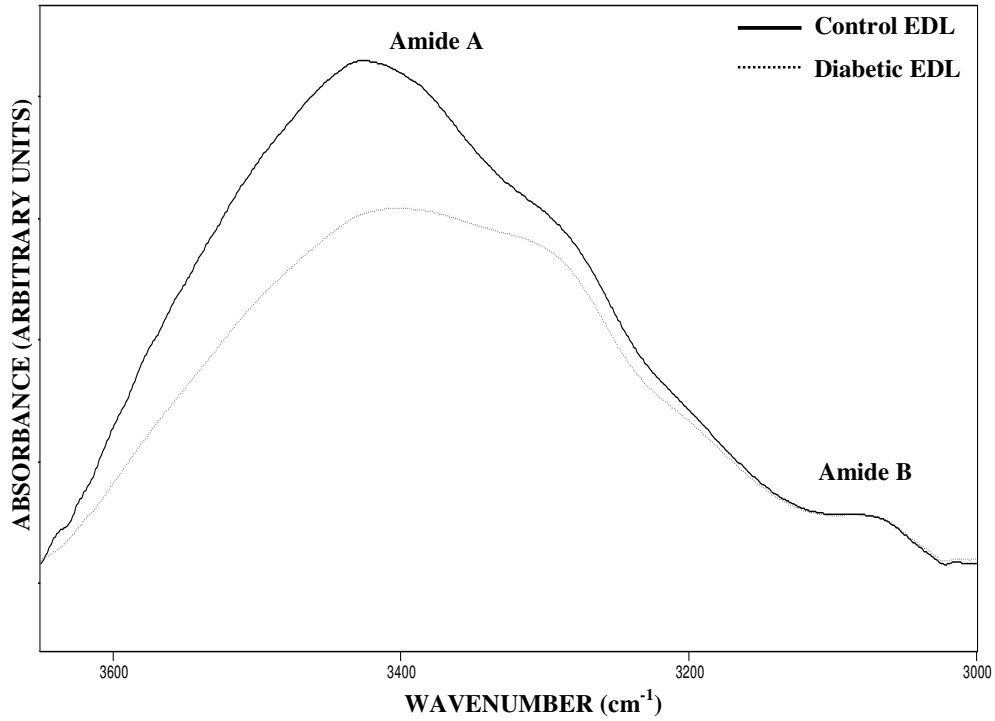

Figure 16. The representative infrared spectra of control and diabetic EDL muscles in the 3650-3000 cm^{-1} region. (The spectra were normalized with respect to the CH_2 asymmetric stretching mode at 2925 cm^{-1})

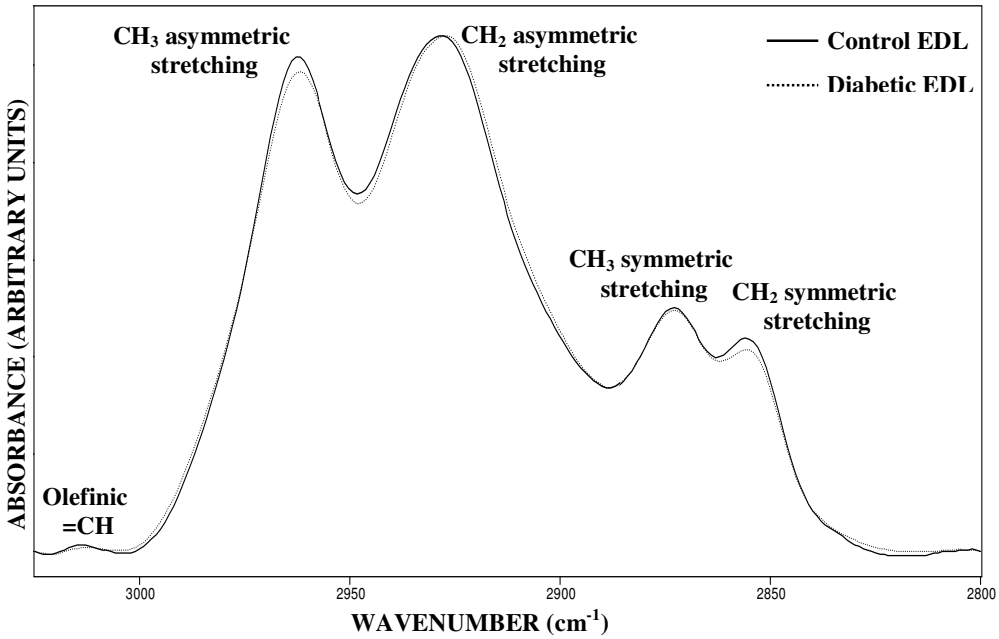

Figure 17. The representative infared spectra of control and diabetic EDL muscle in the 3025-2800 cm^{-1} region. (The spectra were normalized with respect to the CH_2 asymmetric stretching mode at 2925 cm^{-1})

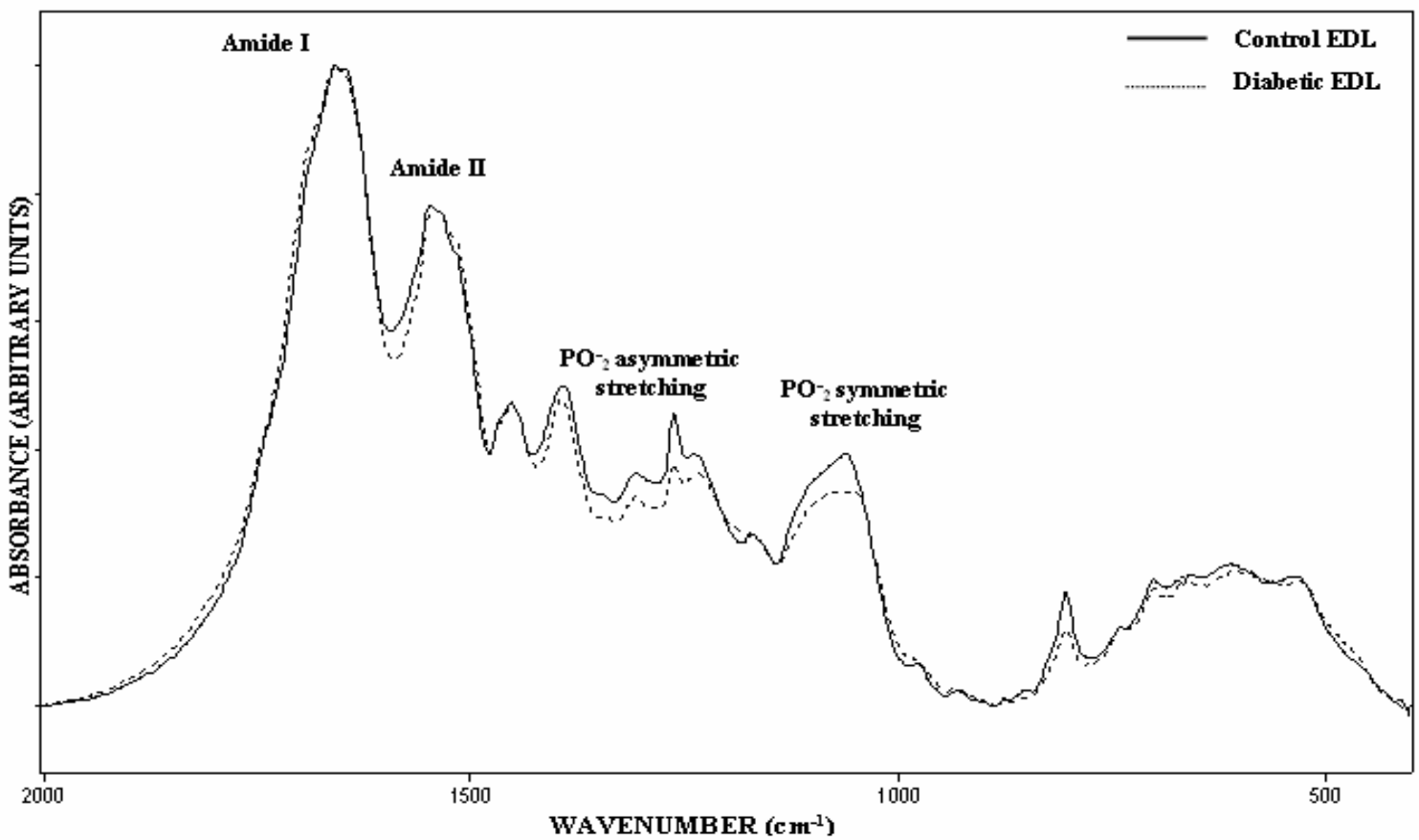

Figure 18. The representative infared spectra of control and diabetic EDL in the 2000-400 cm^{-1} region. (The spectra were normalized with respect to the Amide I at 1645 cm^{-1})

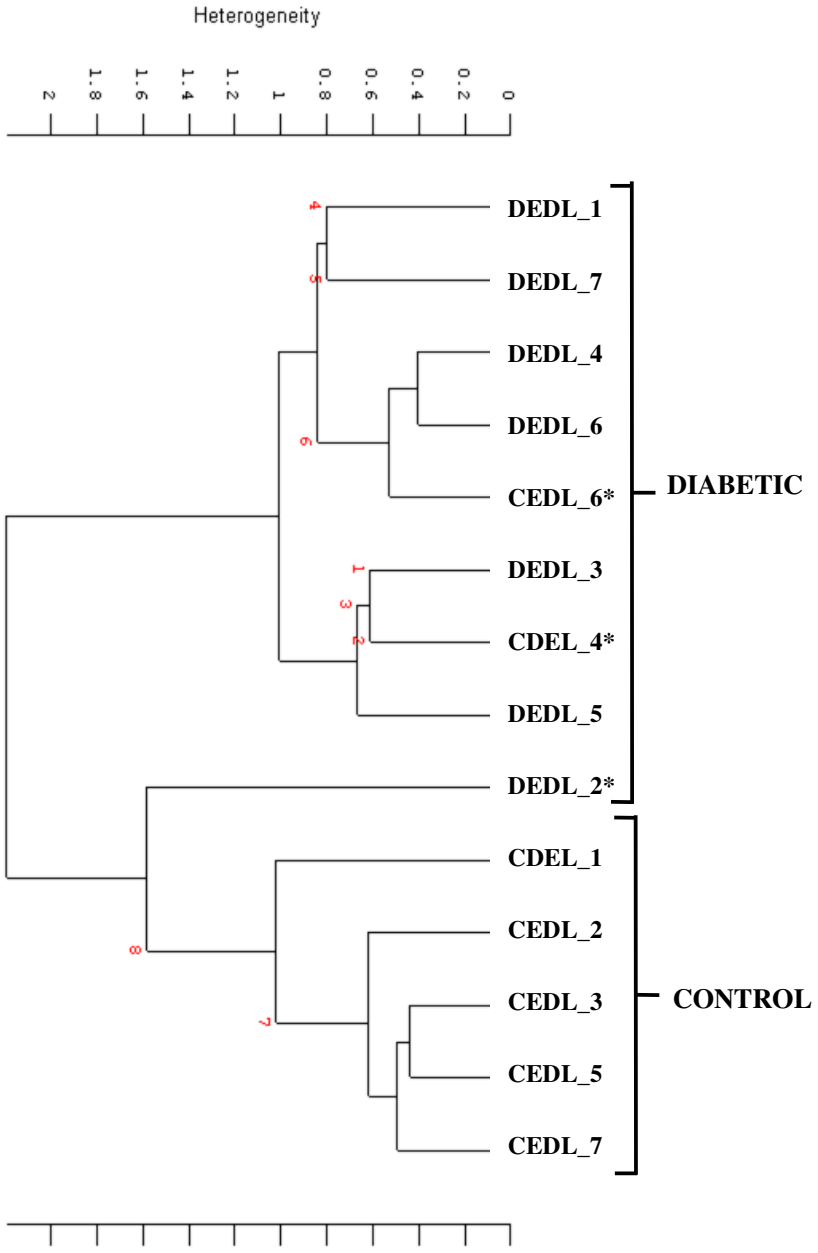

Figure 19. Hierarchial clustering of control and diabetic EDL muscles using second derivative spectra (spectral range: 4000-400 cm^{-1}). The samples labelled with * were not clearly differentiated, and not used in statistical analysis.

3.2.3 Numerical Comparisons of the Bands of Control and Diabetic Spectra of EDL and SOL Muscles

In order to take the possible spectral differences that could be observed between the individuals of even same group into account, the means and the standard deviations of the band areas and direction of the shifts with respect to control were obtained for control and diabetic groups of both EDL and SOL muscle. Diabetic group-means of each muscle type were compared with those of control group-means with the help of Mann-Whitney U-test and significance values were calculated. The results of changes in frequency values were given in Table 2 and changes in band areas were given in Table 3. The changes in bandwidth values were presented in Table 4. The results revealed that the changes in the spectral parameters for both muscle types were in the same direction.

Table 2. Numerical summary of the detailed differences in the band frequencies of control and diabetic spectra. The values are the mean ± Standart Deviation for each sample. The degree of significanca was denoted as $p<0.05$*, $p<0.01$**, $p<0.001$***.

	BAND FREQUENCY			
Band No	**Control EDL (n=5)**	**Diabetic EDL (n=6)**	**Control SOL (n=6)**	**Diabetic SOL (n=6)**
2	3399.43 ± 23.62	3385.79 ± 25.30↓	3371.87 ±27.38	3337.68± 11.71*↓
3	3071.02 ± 1.02	3072.39 ± 1.57 ↑	3071.37 ± 1.34	3073.38 ± 3.45↑
4	3015.38 ± 3.64	3014.25 ± 0.93↓	3011.97 ± 0.85	3014.13 ±1.17**↑
5	2962.52 ± 0.41	2962.70 ± 0.43↑	2962.02 ± 0.22	2962.60 ±0.23**↑
6	2929.23 ± 0.54	2927.77 ±0.81**↓	2929.27 ± 0.46	2929.06 ± 1.25↓
7	2873.78 ± 0.46	2874.58 ± 0.75↑	2874.12 ± 0.21	2874.37 ± 0.60↑
8	2854.95 ± 0.09	2855.70 ± 0.38**↑	2855.66 ± 0.30	2855.09 ± 0.40*↓
9	1655.75 ± 1.05	1656.7 ± 4.68↑	1656.76 ± 0.91	1658.15 ± 1.72↑
10	1540.04 ± 0.45	1536.02 ± 4.87*↓	1540.13 ± 0.55	1538.96 ±1.11↓
11	1453.13 ± 1.10	1454.76 ± 3.06↑	1451.19 ± 0.19	1452.58 ±0.89**↑
12	1392.56 ± 1.02	1393.23 ± 2.65↑	1392.99 ± 0.20	1393.66 ± 1.00↑
13	1343.92 ± 0.59	1343.05 ± 2.62↓	1345.29 ± 0.31	1344.17 ±0.87*↓
14	1261.18 ± 0.42	1261.55 ± 0.30↑	1260.09 ± 0.49	1260.91 ± 0.88↑
15	1236.52 ± 1.80	1233.88 ± 1.19*↓	1238.40 ± 0.63	1234.93 ±2.00**↓
16	1169.98 ± 0.45	1169.99 ± 2.04↑	1171.30 ± 0.40	1170.78 ± 0.85↓
17	1068.03 ± 5.03	1066.82 ± 4.91↓	1081.60 ± 1.65	1069.15 ±5.35**↓
18	978.19 ± 2.03	981.12 ± 1.72↓	978.33 ± 1.17	979.14 ± 2.63↑
19	872.66 ± 0.79	873.51 ± 0.36↑	873.22 ± 0.76	873.75 ± 0.37↑
20	802.98 ± 0.11	803.22 ± 0.30↑	802.28 ± 0.84	802.68 ± 0.48↑

Table 3. Numerical summary of the detailed differences in the band areas of control and diabetic spectra. The values are the mean ± Standart Deviation for each sample. The degree of significanca was denoted as $p<0.05$*, $p<0.01$**, $p<0.001$***.

	BAND AREA			
Band No	**Control EDL (n=5)**	**Diabetic EDL (n=6)**	**Control SOL (n=6)**	**Diabetic SOL (n=6)**
2	49.18 ± 9.50	36.76 ± 8.51↓	69.31 ± 8.81	47.17 ± 15.56*↓
3	5.52 ± 1.28	4.40 ± 1.29↓	9.58 ± 1.27	6.00 ± 1.98**↓
4	1.18 ± 0.28	0.93 ± 0.27↓	1.87 ± 0.24	1.25 ± 0.39*↓
5	3.71 ± 0.93	2.84 ± 0.81↓	5.80 ± 0.78	3.87 ± 1.29*↓
6	4.07 ± 1.00	3.18 ± 0.88↓	6.40 ± 0.82	4.33 ± 1.37*↓
7	1.30 ± 0.30	1.00 ± 0.27↓	1.89 ± 0.23	1.38 ± 0.41*↓
8	1.12 ± 0.25	0.83 ± 0.22↓	1.69 ± 0.19	1.07 ± 0.29**↓
9	16.79 ± 5.73	12.05 ± 4.16↓	31.20 ± 5.01	17.96 ± 8.17**↓
10	11.04 ± 3.73	7.66 ± 2.66↓	20.22 ± 3.23	11.62 ± 5.02**↓
11	3.33 ± 0.87	2.88 ± 0.86↓	4.98 ± 0.60	3.59 ± 1.10**↓
12	4.59 ± 1.23	3.35 ± 1.01↓	6.94 ± 0.86	4.57 ± 1.51**↓
13	0.96 ± 0.25	0.82 ± 0.24↓	1.45 ± 0.17	1.25 ± 0.40↓
14	1.77 ± 0.44	1.45 ± 0.39↓	2.18 ± 0.26	1.79 ± 0.58↓
15	3.06 ± 0.82	2.35 ± 0.69↓	4.96 ± 0.62	3.38 ± 1.08**↓
16	1.51 ± 0.39	1.18 ± 0.30↓	2.12 ± 0.24	1.48 ± 0.45**↓
17	6.16 ± 1.17	5.41 ± 1.00↓	7.44 ± 0.71	6.26 ± 1.62↓
18	0.30 ± 0.07	0.30 ± 0.05	0.42 ± 0.05	0.31 ± 0.07*↓
19	0.02 ± 0.01	0.03 ± 0.02↑	0.01 ± 0.00	0.03 ± 0.01*↑
20	0.56 ± 0.07	0.53 ± 0.09↓	0.64 ± 0.07	0.59 ± 0.18↓

Table 4. Numerical summary of the detailed differences in the bandwidths of control and diabetic spectra. The values are the mean ± Standart Deviation for each sample. The degree of significanca was denoted as $p<0.05$*, $p<0.01$**, $p<0.001$***.

	BANDWIDTH			
Band Name	**Control EDL (n=5)**	**Diabetic EDL (n=6)**	**Control SOL (n=6)**	**Diabetic SOL (n=6)**
CH_3 asym	8.44 ± 0.13	8.35 ± 0.41↓	8.85 ± 0.28	8.65 ± 0.16↓
CH_2 asym	9.47 ± 0.31	10.03 ± 0.41↑	9.76 ± 0.19	9.99 ± 0.19↑
Amide I	30.20 ± 1.70	30.40 ± 2.6↑	27.40 ± 2.60	31.20 ± 2.50*↑
Amide II	28.10 ± 0.70	34.80±4.6**↑	27.50 ± 0.40	32.10 ± 4.50*↑

3.3 Detailed Spectral Analysis

3.3.1 Comparison of Control and Diabetic Spectra of SOL and EDL Muscles in 3600-2800 cm^{-1} Region

As seen from Figures 12, 13, 16 and 17, the 3600-2800 cm^{-1} region contains several bands. The bands centered at 3360 cm^{-1} (Amide A) and 3068 cm^{-1} (Amide B) correspond to the OH and/or the NH stretching mode, the NH and/or the CH vibrations, respectively. The band centered at 3014 cm^{-1} monitors stretching mode of the H-C=C-H vibrations. The other bands between 3000-2800 cm^{-1} are in the C-H region. These bands are centered at 2959 cm^{-1}, 2927 cm^{-1}, 2876 cm^{-1} and 2857 cm^{-1}, and they monitor both the CH_3 and the CH_2 asymmetrical, and both the CH_3 and the CH_2 symmetrical vibrations, respectively (Melin *et* al., 2000; Chang and Tanaka, 2002; Çakmak *et al.*, 2003; Severcan *et al.*, 2003, Cakmak *et al.*, 2006).

Figure 12 and Figure 16 shows the normalized infrared spectra of control and diabetic SOL and EDL muscles, respectively, in 3600-3050 cm^{-1} region. The band located at 3360 cm^{-1} (Amide A) contains strong absorptions arising from the N-H and the O-H stretching modes of proteins and polysaccharides (Melin *et al.*, 2000; Cakmak *et al.*, 2006). As it can be seen from the Figures there is a reduction in the area of this band for both muscle types, more profoundly for SOL muscle ($p<0.05$*). The frequency of the Amide A band shifted slightly to

a lower value in diabetic EDL muscle from 3399.43 ± 23.62 cm^{-1} to 3385.79 ± 25.30 cm^{-1}, but this change was insignificant. However, in diabetic SOL muscle the frequency of this band shifted to a higher value from 3371.87 ± 27.38 cm^{-1} to 3337.68 ± 11.71 cm^{-1} ($p<0.05$*).

Figure 13 and 17 shows the normalized infrared spectra of control and diabetic SOL and EDL muscles in 3025-2800 cm^{-1} region, respectively. The intensity of the band located at 3015 cm^{-1}, which is due to the CH stretching mode of the HC=CH groups, can be used as a measure of unsaturation in the phospholipid acyl chains (Takahaski *et al*., 1991; Melin *et al*., 2000; Liu *et al.*, 2002; Severcan *et al.*, 2005). There was a decrease in the area of this band for both muscle types, and the decrease was more profound for SOL muscle ($p<0.05$*). A more clear representation of the change in areas of both muscles is shown in Figure 20. The frequency of the band located at 3014 cm^{-1} shifted slightly to a lower value in diabetic EDL muscle from 3015.38 ± 3.64 cm^{-1} to 3014.25 ± 0.93 cm^{-1}, but this change was insignificant. However, in diabetic SOL muscle the frequency of this band shifted to a higher value from 3011.97 ± 0.85 cm^{-1} to 3014.13 ± 1.17 cm^{-1} ($p<0.01$**).

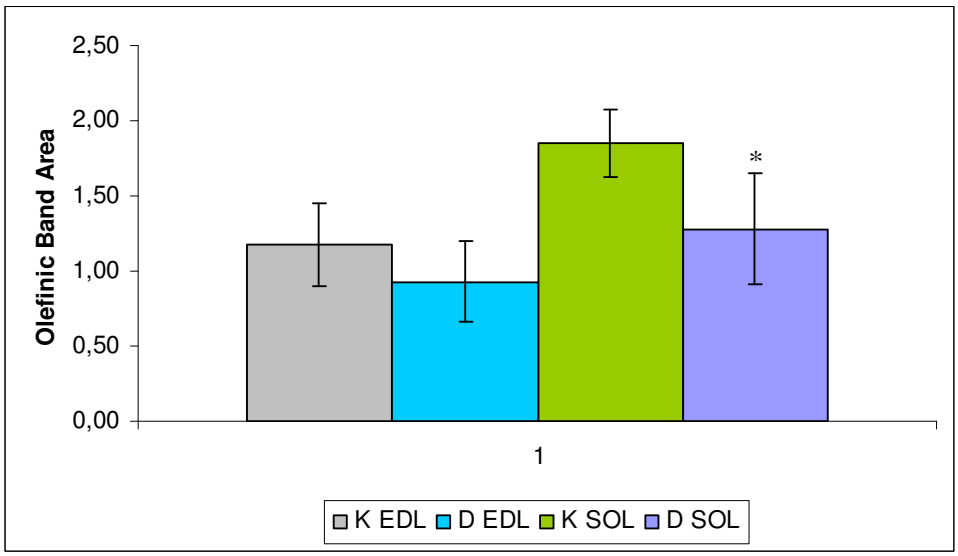

Figure 20. Comparison of =CH olefinic band area for control and diabetic groups of EDL and SOL muscles. ** shows a significance of $p<0.01$

The CH_3 asymmetric (2959 cm^{-1}), the CH_2 asymmetric (2927 cm^{-1}), and the CH_2 symmetric (2857 cm^{-1}) stretching bands originate mainly from lipids, whereas the the CH_3 (2876 cm^{-1}) symmetric stretching band originate mainly from proteins (Mantsch, 1984; Severcan *et al*. 1997; Severcan *et al.*, 2000; Severcan *et al.*, 2003, Cakmak *et al.*, 2006).

In diabetic groups of both muscle types there was a reduction in the areas of the CH_3 asymmetric and symmetric stretching vibrations more profoundly for diabetic SOL muscle ($p<0.05$*). The frequency of this band in diabetic groups shifted to higher frequency values for both muscle types, but the shift was more dramatic for the diabetic SOL muscle ($p<0.01$**). Also the area of CH_3 symmetric stretching vibration decreased in both muscle types, more profoundly for diabetic SOL muscle ($p<0.05$*).

The CH_2 stretching vibrations depend on the degree of conformational disorder; hence they can be used to monitor the average trans/gauche isomerization in the system (Mantsch *et al.*, 1984; Severcan, 1997; Bizeau *et al.*, 2000). As a consequence they increase with the introduction of gauche conformers in the fatty acyl chains (Rana *et al.*, 1990; Schultz *et al.*, 1991; Melin *et al.*, 2000; Çakmak *et al.*, 2003; Cakmak *et al.*, 2006)

As seen from Figures 13 and 17, the areas of the CH_2 asymmetric and symmetric stretching vibrations located at 2929 cm^{-1} and 2855 cm^{-1} respectively, decreased in diabetic groups of both muscle types. This decrease was more profound for SOL muscle in both bands ($p<0.01$**). The frequency of CH_2 asymmetric stretching band shifted to a lower frequency value in diabetic EDL muscle from 2929.23 ± 0.54 cm^{-1} to 2927.77 ± 0.81 cm^{-1}, with a significance value of $p<0.01$**. In diabetic SOL muscle the frequency of this band shifted slightly to a lower frequency value from 2929.27 ± 0.46 cm^{-1} to 2929.06 ± 1.25 cm^{-1}, and the change is insignificant. The frequency of the CH_2 symmetric stretching band shifted to a higher frequency value in EDL muscle ($p<0.01$**), whereas the frequency of this band very slightly shifted to lower frequency values in SOL muscle. No significant change was observed in the bandwidth of the CH_2 asymmetric stretching band in diabetic groups of both muscles as presented in Table 4.

The amount of proteins and lipids in the membranes is an important factor affecting the membrane structure and dynamics (Szalontai *et al.*, 2000). From the FTIR spectrum, a precise lipid-to-protein ratio can be derived by calculating the ratio of the areas of the bands arising from lipids and proteins. As it is seen from Table 5 the ratio of the area of the CH_2 asymmetric stretching band to the area of the CH_3 symmetric stretching band which gives lipid-to-protein ratio was lower in both diabetic muscles, more profoundly for diabetic SOL muscle ($p<0.01$**). The lipid-to-protein ratio calculated as the ratio of the sum of the areas of the CH_2 asymmetric and symmetric stretching bands to the area of the CH_3 symmetric stretching band was also lower in both diabetic muscle types, more profoundly for diabetic SOL muscle ($p< 0.05$*).

Table 5. Numerical summary of the detailed differences in the lipid-to-protein ratios of control and diabetic spectra. The values are the mean ± Standart Deviation for each sample. The degree of significanca was denoted as $p<0.05$*, $p<0.01$**, $p<0.001$***.

Ratio of Peak Areas (lipid to protein)	Control EDL (n=5)	Diabetic EDL (n=6)	Control SOL (n=6)	Diabetic SOL (n=6)
CH_2 Asym. / CH_3 Sym.	3.28 ± 1.04	3.17 ± 0.06↓	3.38 ± 0.03	3.04 ± 0.10**↓
CH_2 Sym. / CH_3 Sym.	0.90 ± 0.27	0.83 ± 0.01↓	0.90 ± 0.13	0.88 ± 0.49↓
CH_2 Asym.+ CH_2 Sym. / CH_3 Sym.	4.19 ± 1.22	3.25 ± 0.98↓	4.27 ± 0.05	3.92 ± 0.48*↓

3.3.2 Comparison of Control and Diabetic Spectra of SOL and EDL Muscles in 2000-400 cm^{-1} Region

The second frequency range under consideration was that of 2000-400 cm^{-1} region. The 2000-400 cm^{-1} frequency range, which corresponds to the fingerprint region, includes several bands that originate from the interfacial and head-group modes of the membrane lipids and from the protein and nucleic acid vibrational modes (Mendelsohn and Mantsch, 1986). Figure 14 and Figure 18 demonstrate the normalized infrared spectra of control and diabetic SOL and EDL muscles in 2000-800 cm^{-1} region, respectively.

The band centered at 1739 cm^{-1} is mainly assigned to the >C=O ester stretching vibration in phospholipids (Melin *et al.*, 2000; Çakmak *et al.*, 2003, Severcan *et al.*, 2003). This band was absent in control and diabetic groups of both muscle types.

The bands at 1656 and 1540 cm^{-1} are attributed to the amide I and II vibrations of structural proteins. The band centered at 1656 cm^{-1} (amide I) corresponds to the C=O stretching and the C-N stretching (% 60) vibrational modes weakly coupled with the N-H bending (% 40) of the polypeptide and protein backbone and the band located at 1540 cm^{-1} (amide II) is assigned to the N-H bending (% 60) and the C-N stretching (% 40) modes of proteins (Melin *et al.*,2000;

Takahashi *et al.*, 1991; Wong *et al.*, 1991; Haris and Severcan, 1999; Çakmak *et al.*, 2003). The band areas of amide I and amide II bands decreased in diabetic groups of both muscles, but the decrease was more dramatic in SOL muscle in both bands ($p<0.01$**). There was a significant shift in the frequency of amide II band to lower values for both diabetic muscles ($p<0.05$*), from 1540.04 ± 0.45 cm^{-1} to 1536.02 ± 4.87 cm^{-1} in EDL muscle and from 1540.13 ± 0.55 cm^{-1} to 1538.96 ± 1.11 cm^{-1} in SOL muscle. As it can be seen from Table 4, there was a broadening in the bandwidth of amide I band for both diabetic muscles, more profoundly for SOL muscle ($p<0.05$*). Moreover, the broadening in the bandwidth of amide II band of both muscle types can be clearly seen from Table 4 and Figures 14 and 18 ($p<0.05$* for SOL , and $p<0.01$** for EDL).

A decrease in the area of the intense band at 1452 cm^{-1}, which is assigned to the CH_2 bending mode of protein and lipids (Manoharan *et al.*, 1993; Çakmak *et al.*, 2003) was observed for diabetic groups of both muscles. The decrease was more dramatical in SOL muscle ($p<0.01$*). As seen from Table 2, there was a shift to higher values in the frequency of this band in diabetic groups of both muscle types, more profoundly for SOL muscle ($p<0.01$**). We observed a decrease in the area of the band at 1392 cm^{-1} which is due to the COO^- symmetric stretching vibration of amino acid side chains and fatty acids (Jackson *et al.*, 1998; Çakmak *et al.*, 2003; Cakmak *et al.*, 2006) in diabetic groups of both muscles, which was more obvious for SOL muscle ($p<0.01$**).

The absorbtion bands of collagen are seen in a broad range in the spectrum. The main bands of collagen arise from peptide bond vibrations detected in amide A, I, II and III bands (Camacho *et al.*, 2001). The amide III vibrations of collagen are seen in the spectral range between 1355 and 1167 cm^{-1} (Gough et al., 2003). The band located at 1343 cm^{-1} falls into this region of the Amide III vibrations, more specifically it originates from the C-N and the C-C stretching and the N-H bending vibrations of collagen (Camacho *et al.*, 2001, Gough *et al.*, 2003; West *et al.*, 2004). As it can be seen from Table 2 the frequency of the band located at 1343 cm^{-1} shifted to lower frequency values in diabetic groups of both muscle types, where the shifting was remarkable for SOL

muscle ($p<0.05$*). There was no significant change in the area of this band in both diabetic muscles.

In the 1280-900 cm^{-1} frequency range, several macromolecules (e.g. polysaccharides and phosphate carrying compounds such as phospholipids and nucleic acids) give absorbtion bands (Melin *et al.*, 2000; Çakmak *et al.*, 2003). The relatively strong bands at 1261, 1236 and 1080 cm^{-1} are mainly due to the asymmetric and symmetric stretching modes of phosphodiester groups, the P=O bond present in the phosphate moieties (PO_2^-) of nucleic acid backbone structures and phospholipids (Wong *et al.*, 1991; Wang *et al.*, 1997; Diem *et al*, 1999; Çakmak *et al.*, 2003). The band located at 1261 cm^{-1} is due to non-hydrogen-bonded PO_2^- groups and the band located at 1236 cm^{-1} is due to more hydrogen-bonded PO_2^- groups (Rigas *et al.*, 1990; Wong *et al.*, 1991). There was a slight decrease in the area of 1261 cm^{-1} band in both muscles, which was not significant. The area of the band located at 1236 cm^{-1} decreased in diabetic SOL muscle ($p<0.01$**). The frequency of the band located at 1261 cm^{-1} shifted slightly to higher values in both diabetic muscles. However, the shift in the frequency of the band located at 1236 cm^{-1} to lower values was from 1236.52 ± 1.80 cm^{-1} to 1233.88 ± 1.19 cm^{-1} in EDL muscle ($p<0.05$*) and from 1238.40 ± 0.63 cm^{-1} to 1234.93 ± 2.00 cm^{-1} in SOL muscle ($p<0.01$**).

The PO_2 symmetric stretching band is generally assigned to be located at 1080 cm^{-1} (Lyman *et al.*, 2001; Banyay *et al.*, 2003). However, the frequency of this band in EDL muscle samples appeared approximately at 1068 cm^{-1}. Also there was a shift to lower values in the frequency of this band in both muscles, especially for SOL ($p<0.01$**). There was an insignificant decrease in the area of the PO_2 symmetric stretching band observed in both muscles. It has been reported that the PO_2 symmetric stretching band might be masked by spectral contributions of glycogen, which exhibits three strong peaks at 1042, 1080 and 1152 cm^{-1} (Chiriboga *et al.*, 2000; Cakmak *et al.*, 2006). Nevertheless, in our spectra this band appeared having shoulders. The band at 1044 cm^{-1} was more apparent to study. It is assigned as mainly to the C-O stretching vibrations of polysaccharides (Melin *et al.*, 2000; Toyran *et al.*, 2006; Cakmak *et al.*, 2006).

We observed a decrease in this band, which was more easily observed in SOL muscle.

The DNA to protein ratio calculated by the ratio of the area of PO_2 symmetric stretching band to the area of amide II band was given in Table 6. As seen from the Table there was an increase in this ratio in both diabetic groups, more profoundly for SOL muscle ($p<0.05$*).

Table 6. Numerical summary of the detailed differences in the DNA to protein ratio of control and diabetic spectra. The values are the mean ± Standart Deviation for each sample. The degree of significanca was denoted as $p<0.05$*, $p<0.01$**, $p<0.001$***.

Ratio of Peak Areas (DNA to protein)	**Control EDL (n=5)**	**Diabetic EDL (n=6)**	**Control SOL (n=6)**	**Diabetic SOL (n=6)**
PO_2 sym./ Amide II	0.61 ± 0.25	0.76 ± 0.20↑	0.37 ± 0.06	0.63 ± 0.34*↑

We observed a significant ($p<0.01$**) decrease in the area of the relatively weak band centered at 1170 cm^{-1}, which is due to asymmetric stretching mode of the CO-O-C groups present in glycogen and nucleic acids (Rigas *et al.*, 1990; Cakmak *et al.*, 2006) for SOL muscle.

The band centered at 976 cm^{-1} is generally assigned to symmetric stretching mode of dianionic phosphate monoester of cellular nucleic acids (Ci *et al.*, 1999; Chiriboga *et al.*, 2000; Çakmak *et al.*, 2003) and ribose-phosphate main chain vibrations of the RNA backbone (Banyay *et al.*, 2003, Tsuboi *et al.*, 1969). There was a significant decrease in the area of this band in diabetic SOL muscle ($p<0.01$*).

The bands centered at 873 cm^{-1} and 802 cm^{-1} both originate from the vibrations of N-type sugars in the sugar phosphate backbone of nucleic acids (Banyay *et al.*, 2003, Taillandier and Liquier, 1992). The 802 cm^{-1} band is also coupled with furanose-phosphodiester chain vibrations (Banyay *et al.*, 2003). There was a slight increase in the area of the band located at 873 cm^{-1} in diabetic SOL

muscle ($p<0.05$*). No significant change was observed in the change in the area of 802 cm^{-1} band.

No significant change was also observed in the frequency changes of 976 cm^{-1}, 873 cm^{-1} and 802 cm^{-1} bands for both muscle types.

CHAPTER 4

DISCUSSION

In the present study FTIR spectroscopic technique had been used to investigate the effects of Type I Diabetes Mellitus on structural components of two types of skeletal muscle tissues, namely Soleus (SOL) and Extensor Digitorum Longus (EDL). As it is given in detail in introduction part, skeletal muscle is composed of different fiber types. SOL muscle is largely composed of type I fibers (84% type I, 16% type IIa, 0% type IIb) having a characteristic of slow-contracting oxidative muscle. Whereas EDL is largely composed of type II fibers (3% type I, 57% type IIa, 40% type IIb) having a fast-contracting glycolytic characteristic (Ariano *et al.*, 1973, Delp *et al.*, 1996).

Healthy skeletal muscle can utilize either lipid or carbohydrate fuels and can rapidly change its fuel selection upon the stimulus and energy demands, also depending on its oxidative or glycolytic capacity (Goodpaster and Wolf, 2004, Goodpaster and Brown, 2005). It has been demonstrated that the loss of flexibility of skeletal muscle to switch between lipid and carbohydrate fuels is an important aspect of insulin resistance in type II diabetes and obesity (Goodpaster and Wolf, 2004). Under normal conditions glycogen is the main source of energy in fast- and slow-contracting skeletal muscles. However, type I (oxidative) muscles were shown to exhibit a greater reliance on lipid at resting conditions and during moderate exercise. On the other hand, type II fibers, having glycolytic or less oxidative capacity, rely on carbohydrate fuel for energy generation (Baldwin et al., 1973).

Skeletal muscle is the major tissue determining the glucose homeostasis in the body (DeFronzo *et al.*, 1981). It has been reported that there is a decrease in the

amount of glucose transporters, uptake of glucose and synthesis of glycogen both in type I and II diabetes (DeFronzo *et al.*, 1987, Kern *et al.*, 1990, Ramlal *et al.*, 1989).

Our results are in accordance with these studies mentioned above. Although amide A band located at 3360 cm^{-1} is assigned to absorbtions arising from the N-H and the O-H stretching modes of H_2O, proteins and glycogen, since in our case water was removed by freeze drying its contribution to this band can be neglected. Therefore, this band gives information about the protein and glycogen content. In infrared spectroscopic analysis, the signal intensity and more accurately the band area of the bands in absorbtion spectra, give information about the concentration of related functional groups (Freifelder, 1982; Toyran and Severcan, 2003; Toyran *et al*., 2004). There was a decrease in the area of this band in SOL muscle, suggesting a decrease in glycogen and protein content. This result was further supported by the decrease in the areas of the bands located at 1044 cm^{-1} and 1170 cm^{-1} both originating from glycogen (Lyman *et al.*, 1999; Rigas *et al.*, 1990; Çakmak *et al.*, 2003, Cakmak et al., 2006), and the decreases were more profound for SOL in both bands. The shoulder at approximately 3420 cm^{-1} is assigned to hydrogen-bonded intermolecular the OH groups, and the shoulder at 3307 cm^{-1} is assigned to the N-H stretching mode (Raudenkolb et al., 2003, Nilsson et al., 1991, Melin et al., 2000). As it can be seen from Figure 12 and 16, the decrease in the shoulder at 3420 cm^{-1} in diabetic groups of both muscle types can be explained by the reduced contribution from glycogen the OH absorbtion (Melin et al., 2000; Cakmak et al., 2006). The frequency of the amide A band shifted to a lower value for both skeletal muscles as seen from Table 2, but more profoundly for SOL muscle. This shift also suggests the decrease in the contribution from glycogen the OH absorbtion. When taken together these results suggest that there is a decrease in the glycogen content in type I diabetes, more profoundly for SOL muscle. He *et al.* (2004) have demonstrated that the glycogen content in type I fiber was lower than that of type IIa and IIb fibers in type II diabetes, which further support our findings.

As it can be seen from Figures 13 and 17, the C-H region (3050-2800 cm^{-1}) is populated by absorbtions arising from the C-H stretching vibrations of olefinic=CH, -CH_2 and -CH_3 groups, most of which originate from lipid structures. In diabetic groups of both muscles, there was a decrease in the areas of the CH_3 asymmetric (2962 cm^{-1}), CH_2 asymmetric (2928 cm^{-1}), CH_2 symmetric (2857 cm^{-1}) stretching bands, indicating a decrease in the total lipid content of skeletal muscles (Severcan et al., 2000; Severcan et al., 2003, Cakmak et al., 2006). This decrease in lipid content was further supported by the decrease in the area of the CH_2 bending (1452 cm^{-1}) band originating from lipids (Severcan et al., 2000; Severcan et al., 2003). The decreases in the areas of the lipid bands were more profoundly for diabetic SOL muscle. This prevalent decrease in lipid content may be the result of increased skeletal muscle lipolysis or utilization of lipid sources in diabetic conditions. Stearns et al. (1979) have found that skeletal muscle fat utilization is increased in STZ-induced diabetic rats. It was also demonstrated that glycerol, the indicator of lypolytic activity, increases in type I muscle fibers in diabetes (Chao et al., 1976; Hagstrom-Toft et al., 2002).

Intramyocellular lipid (IMCL) is another energy source for skeletal muscles. There is a close relationship between muscle lipid content and skeletal muscle insulin resistance, which in turn leads to the formation of type II diabetes, reported in many studies (Oakes *et al.*, 1997, He *et al.*, 2001, Goodpaster *et al.*, 2001). In most of the studies lipid and triglyceride content of skeletal muscle was found to be higher in type II diabetic subjects (Lithell *et al.*, 1981, Goodpaster *et.al.*, 1997, Malefant *et al.*, 2001, He *et al.*, 2001). Although there is insulin in circulation in type II diabetes, due to some other factors like insulin resistance, muscles switch their source of fuel from glucose to mainly lipids. Therefore, the intake of non-esterified free fatty acids from circulation, their esterification into triglycerides and intramyocellular storage of lipids increases (Van Loon et al., 2005). IMCL content was also reported to be increased in subjects with type I diabetes (Perseghin *et al.*, 2003, Ebeling *et al.*, 1998). Bernroider *et al.* (2006) studied with type I diabetic subjects and reported that no significant change was observed between diabetic and control group IMCL contents. Hopp and Palmer (1991) studied with diabetic animals

and found no significant effect of diabetes mellitus on triglyceride or lipid content. Therefore, there are some contradictory results about the effect of diabetes on lipid composition of skeletal muscle. Our finding of decrease in lipid content contradicts with some of the studies stated above. Most of the studies concerning the effects of diabetes are clinical studies about type I diabetes that were carried out with human subjects who were given insulin administration daily, which means not a severe diabetic condition is generated. In contrast in our study, rats were not given any insulin administration throughout the six weeks of time, generating a severe and chronic diabetic condition. Jacob et al. (1999) have shown that low physiological dose of insulin suppresses the lipolysis in skeletal muscle and adipose tissue. This finding can explain the increased content of lipids and triglycerides in insulin administration. Moreover, in our study the total lipid content was measured. Our study was first to report the decrease in total lipid content in skeletal muscles of type I diabetic rats, which was more profound for SOL muscle.

The band located at 3015 cm^{-1} is due to the CH stretching mode of the HC=CH groups. Therefore, the intensity of this band can be used as a measure of unsaturation in the acyl chains (Takahashi *et al.*, 1991, Liu *et al.*, 2002; Severcan *et al.*, 2005). As seen from Figure 20, the area of this band decreased in diabetic groups of both muscles, more profoundly for SOL muscle, indicating the decrease in the population of unsaturation in acyl chains of lipid molecules. This loss of unsaturation might have been caused by the increase in lipid peroxidation (Sills *et al.*, 1994; Kinder et al., 1997). This result is in accordance with Arango *et al.* (2004), that hydrogen peroxide production, an end product of lipid peroxidation, is increased in skeletal muscles of STZ-induced diabetic rats. Type I fibers rely on oxidative pathway to utilize fuels, and have a high content of mitochondria (Armstrong et al., 1975; Chao et al., 1976; Armstrong et al., 1977). Both of these properties of type I fibers make them susceptible to the increased ROS production, as mitochondria provide most of the energy in these fibers and ROS production generally occurs in the inner membrane of mitochondria where the electron transport chain is present (West, 2000; Leary et al., 2003). Leary et al. (2003) demonstrated that ROS production is increased in slow-contracting type I muscle fibers. Hence, lipid

peroxidation was increased in diabetic skeletal muscles due to the increased production of ROS in diabetes. SOL muscle, which is composed of a greater percent of type I fibers, was more affected from lipid peroxidation when compared with EDL muscle.

In addition to the decrease in intensity, there was a frequency shift to higher frequency values for the olefinic band in SOL muscle. In the previous studies, the frequency shift to lower values was reported as to be an indication of an increase in order of the system (Mantsch, 1984; Lopez-Garcia *et al.*, 1993; Bizeau *et al.*, 2000; Severcan et al., 2003). However, in our study the shift to higher values was observed in olefinic =CH stretching band representing the disordering of the unsaturated lipids in membranes of skeletal muscle tissue. This disordering of the membrane unsaturated lipids can be a result of lipid peroxidation. Since SOL muscle was more affected from lipid peroxidation, the degree of disordering of the unsaturated lipids was also higher in this fiber type. This study was first to report this disordering of unsaturated lipids in diabetes.

The shift to lower frequencies of the CH_2 stretching vibrations can be used as a marker for the detection of increased lipid order (Liu *et al*. 2002; Mantsch, 1984; Severcan *et al*. 1997). In our study the frequency of the CH_2 asymmetric stretching band shifted to lower values in diabetic groups of both muscles, but the shifting was more profound for EDL muscle. This shifting demonstrates an increase in the order of the system, which indicates an increase in the number of trans conformers resulting in more rigid membranes. A possible explanation for the membrane rigidity is the free radicals, and consequently the lipid peroxidation, which modifies the lipid composition of the membranes. After oxidative stress, a decrease in the membrane unsaturated/saturated fatty acid ratio is detected along with the formation of cross-linked lipid–lipid and lipid–protein moieties (Curtis *et al*., 1984; Levin *et al*., 1990; Niranjan and Krishnakantha, 2000). The altered unsaturated/saturated fatty acid ratio of membrane phospholipids evidently result with the increase in rigidity of membrane.

Membrane fluidity is detected by monitoring the bandwidth of the C-H stretching bands (Mantsch, 1984; Lopez-Garcia et al., 1997; Severcan *et al*., 2003; Severcan *et al.*, 2005). The increase in the bandwidth corresponds to an increase in membrane fluidity (Levin *et al*., 1990; Severcan et al., 1999; Severcan et al., 2005; Korkmaz and Severcan, 2005). As seen from Table 4, no significant change was observed in the CH_2 asymmetric stretching bandwidth values of EDL and SOL muscles of diabetic rats.

The band centered at 1739 cm^{-1} is mainly assigned to the >C=O ester stretching vibration in triglycerides (Nara *et al.*,2002; Voortman *et al.*,2002; Çakmak *et al.*, 2003; Cakmak *et al.*, 2006). Although this band was present in the control and diabetic absorbtion spectra of both muscles, the band was seen as a very small broad shoulder, which disabled us to carry out detailed spectral analysis. Due to this reason no assumption can be made considering triglyceride content and structure in diabetic muscles.

The band centered at 1656 cm^{-1} (amide I) corresponds to the C=O stretching and the C-N stretching (% 60) vibrational modes weakly coupled with the N-H bending (% 40) of the polypeptide and protein backbone and the band located at 1540 cm^{-1} (amide II) is assigned to the N-H bending (% 60) and the C-N stretching (% 40) of proteins (Melin et al.,2000; Takahashi et al., 1991; Wong et al., 1991; Cakmak *et al.*, 2006). As it can be seen from Table 3 and Figures 14 and 18, there was a decrease in the areas of amide I and amide II bands in diabetic groups of both muscles, more profoundly for SOL, indicating a decrease in total protein content of skeletal muscle in diabetic conditions especially in slow-contracting oxidative muscles. The bands located at 3360 cm^{-1} and 3068 cm^{-1} contain strong absorptions arising from the N-H and the O-H stretching modes of proteins and polysaccharides, and the NH and/or CH vibrations from proteins, respectively (Melin et al., 2000, Chang and Tanaka, 2002). There was a decrease in the areas of both bands in diabetic groups of both muscles, especially for SOL muscle, supporting the decrease in total protein content in diabetic conditions. This decrease was further supported by the decrease in the area of the CH_3 symmetric (2876 cm^{-1}) stretching band which originates mainly from proteins, more profoundly for SOL muscle. It

has been demonstrated that there is an increase in protein breakdown in skeletal muscles accompanied by no increase in muscle protein synthesis in type I diabetic patients (Charlton and Nair, 1998). Insulin stimulates the uptake of a number of amino acids into the muscle cell, so reduced availability of essential amino acids for protein synthesis may be a factor of diabetic myopathy (Wool et al., 1968; Armstrong and Ianuzzo, 1977).

The band at 1392 cm^{-1} is due to the COO^- symmetric stretching vibrations of amino acid side chains and fatty acids (Jackson *et al.*, 1998; Çakmak *et al.*, 2003). The decrease in the area of this band indicates a decrease in the content of amino acids and fatty acids, which is consistent with the other finding of our study stated above.

The ratio of the sum of the areas of the CH_2 asymmetric and symmetric stretching bands to the area of the CH_3 symmetric stretching band decreases in diabetic groups of both muscles, more profoundly for SOL muscle (Table 5). As it was given above, a decrease in protein and lipid contents of skeletal muscle were both observed. Therefore, the decrease in lipid-to-protein ratio suggests that there was a more pronounced decrease in lipid content when compared to the decrease in protein content.

Since the frequency of vibration of amide I band is sensitive to protein conformation, this band is very useful for determination of protein secondary structure (Haris and Severcan, 1999; Jackson *et al.*, 1999, Lyman *et al.*, 1999). A very slight shift to lower values was observed in the frequency of amide I band in diabetic groups of both muscles. In addition there was a significant shift to lower values in the frequency of amide II band, observed both in diabetic EDL and SOL muscles. This shift was to lower frequency values from 1540 cm^{-1} to 1536 cm^{-1} in EDL muscle and from 1540 cm^{-1} to 1539 cm^{-1} in SOL muscle. Amide II band also gives information about protein secondary structure. The band around 1544 cm^{-1} is assigned to α-helix structures of proteins and the shift to lower frequency values, as in our case, indicate an increase in content of random coil structures (Melin *et al.*, 2000; Spassov *et al.*, 2006; Dousseau and Pezolet, 1990). The changes in band positions of both

amide I and amide II bands, indicate a change in protein structure and conformation. The changes in bandwidth of amide I band provide information about protein conformation in the system. There was a broadening in the bandwidth of amide I band, especially for SOL muscle, suggesting that conformational changes in protein structures have occurred in diabetic conditions. Moreover, as seen from Table 4, the bandwidth of amide II band have also increased for diabetic EDL and SOL muscles, supporting the altered protein structure. This result is further important, because the changes in protein secondary structures were reported in this current study for the first time.

The band located at 1343 cm^{-1} originates from the C-N and the C-C stretching and the N-H bending vibrations of collagen (Camacho et al., 2001, Gough et al., 2003; West et al., 2004). The 1365-1300 cm^{-1} spectral region contains bands assigned to plane-bending hydroxyl modes in saccharides (Cael et al., 1973; Carpenter and Crowe, 1989). Therefore, there may have been contributions from saccharide molecules in this band. As it can be seen from Table 3, there was a slight decrease in the area of this band in both diabetic muscles. However, this decrease was not significant. There was a significant shift to lower values in the frequency of this band in diabetic SOL muscle, indicating a structural change in collagen molecules in diabetic type I fibers, which was detected for the first time.

The 1300-1000 cm^{-1} spectral range is commonly coupled with the infrared bands of the stretching modes of the P=O bond present in the phosphate moieties (PO_2^-) of phospholipids and nucleic acids (Diem *et al*, 1999; Liquier and Taillandier, 1996). These phosphate-stretching vibrations are believed to provide valuable information about the head-groups of the phospholipids in the polar-nonpolar interface of membranous structures (Mendelsohn and Mantsch, 1986). Furthermore, these infrared bands can also monitor alterations in the quantity, conformational state, and the degree and position of phosphorylation of the nucleic acids in DNA and RNA (Dovbeshko *et al*, 2000; Kneipp *et al*, 2000). These vibrations are mainly the PO_2 asymmetric and symmetric stretching bands located at 1239 cm^{-1} and 1080 cm^{-1} respectively, originating

from the phosphate-stretching vibrations of nucleic acids and phospholipid head groups (Lyman et al., 2001; Banyay *et al.*, 2003). The frequency of the PO_2 asymmetric stretching mode is at 1240-1260 cm^{-1} when PO_2^- groups are completely non-hydrogen-bonded, and approximately at 1220 cm^{-1} when PO_2^- groups are completely hydrogen bonded (Rigas *et al.*, 1990; Wong *et al.*, 1991). So as the hydrogen bonding increases, the frequency values shift to lower value in PO_2 asymmetric stretching vibration. In the absorbtion spectra of the skeletal muscle, in the region of the PO_2 asymmetric stretching band two bands were observed located at 1261 cm^{-1} and 1236 cm^{-1}. The band located at 1261 cm^{-1} is due to non-hydrogen-bonded PO_2^- groups and the band located at 1236 cm^{-1} is due to more hydrogen-bonded PO_2^- groups. No significant change was observed in the area of the band located at 1261 cm^{-1} in both muscles when compared with controls. However, there was a significant decrease in the area of the band located at 1236 cm^{-1} in diabetic SOL muscle. Moreover, there was a very slight decrease in the area of the PO_2 symmetric stretching band is located at 1080 cm^{-1} in both diabetic muscles. Hence, this result indicates a decrease in the content of nucleic acids and phospholipids in the membrane structures of skeletal muscles, especially in SOL muscle. In addition there was a frequency shift to lower values in the band located at 1236 cm^{-1} in both diabetic muscles. The frequency shift to lower values was also observed in the PO_2 symmetric stretching band located at 1080 cm^{-1}, more profoundly in SOL muscle. Moreover, in the EDL muscle the PO_2 symmetric stretching band was not located at 1080 cm^{-1} as reported in literature; instead it had been located at 1068 cm^{-1}. This shift results from the increased hydration of the nucleic acid and phospholipids in membrane structures (Diem *et al*, 1999; Pevsner and Diem, 2003). All together these results suggest a change in DNA and RNA conformation, possibly by increasing the effect of hydrogen bonding in the DNA and RNA backbones (Dovbeshko *et al*, 2000). A similar interpretation can be made for the phosphate groups in the polar region of the lipid bilayer. Hence, the shift to lower values in the frequency of these bands in diabetes seems to support the ordering effect of diabetes mentioned earlier. These results are further important, since the increase in hydrogen bonding of nucleic acids and phospholipids, and the structural changes in nucleic acids were first to be reported in this current study. It has been demonstrated that diabetes

affected the gene expression of several proteins, glycoproteins and proteoglycans (Lehti et al., 2006), supporting the altered protein expression and nucleic acid content in diabetes. It has also been demonstrated that the expression of glucose transporters decreases in diabetes (Ramlal et al., 1989), supporting our finding that both RNA and protein content decrease in diabetes.

A decrease in both protein and DNA content was observed in diabetes, as seen in Table 6, however this decrease was more profoundly in the protein content when compared with the DNA content.

The spectral region between 995-970 cm^{-1} is assigned to the ribose-phosphate main chain vibrations of RNA (Banyay *et al.*, 2003). The absorbtion bands originating from CC structure of the DNA backbone was assigned to lower frequency values between 970-950 cm^{-1} (Banyay *et al.*, 2003). The band centered at 976 cm^{-1} is generally assigned to symmetric stretching mode of dianionic phosphate monoester of nucleic acids (Ci *et al.*, 1999; Chiriboga *et al.*, 2000; Çakmak *et al.*, 2003) and ribose-phosphate main chain vibrations of the RNA backbone (Banyay *et al.*, 2003, Tsuboi *et al.*, 1969). A decrease in the area of this band was observed in diabetic SOL muscle, indicating a decrease in the nucleic acid, especially RNA content in diabetic SOL muscle. This decrease suggests that the RNA production, therefore the protein synthesis is decreased in diabetic SOL muscle. This result supports the decrease in protein content mentioned earlier. The decrease in protein synthesis might have been caused by alterations in expression of nucleic acids which may be a result of any structural changes in nucleic acid structures.

The bands centered at 873 cm^{-1} and 802 cm^{-1} both originate from the vibrations of N-type sugars in the sugar phosphate backbone of nucleic acids, both DNA and RNA (Banyay *et al.*, 2003, Taillandier *et al.*, 1992). The 802 cm^{-1} band is also coupled with furanose-phosphodiester chain vibrations (Banyay *et al.*, 2003). The slight changes in frequencies of these bands located at 976 cm^{-1}, 873 cm^{-1} and 802 cm^{-1} were not significant in both diabetic EDL and SOL muscle, suggesting little or no change occurred in the structure of backbone structures of DNA and RNA.

There have been controversial results reported in literature concerning the effect of diabetes on skeletal muscle fibers, about their protein and lipid content, and their breakdown or synthesis metabolisms. It has been proposed that slow-contracting muscle fibers are not affected strongly from diabetes when the histochemistry of muscles was examined in diabetic condition (Armstrong et al., 1975; Armstrong et al., 1977). Later on, slow-contracting muscle fibers were reported to have an increased content of insulin-regulated glucose transporters and greater insulin sensitivity for glucose metabolism, therefore; they were reported to be strongly affected from diabetes (He *et al.*, 2001; Kelley and Goodpaster, 2001, Leary et al., 2003). However, our current study clearly showed that SOL muscle, which is composed of a high content of type I fibers, was more severely affected from diabetes in all the spectral parameters stated above.

The present study is further important as it sheds light on the structural alterations occurring in the macromolecular content of diabetic skeletal muscle tissues, which give valuable information for clinical studies. There are aspects yet to be resolved in the etiology of diabetes mellitus, and there is no exact treatment of diabetes except for the daily insulin administration to patients. By the help of the results of this study, treatment strategies for the generation of new drugs can be developed. Moreover, new therapies to reduce the symptoms originating from the complications of diabetes can be designed to help ease the pain of patients. For example, usage of drugs, which balance the hydration of nucleic acids and/or create less rigid membrane structures, and antioxidants, can be encouraged. In addition, results of this study will contribute to the database which can be used as control for rapidly testing the effectiveness of newly developed drugs. Drugs can be accepted as suitable for clinical usage, if they can recover the destructive effects of diabetes on structural components of tissues, a part of which have been demonstrated in the present study.

Early diagnosis currently gains significant importance in rapid treatment of diseases. FTIR is one of the suitable techniques which allow rapid visualization of the presence and state of the diseases depending on specific spectral database. Variations in spectral parameters, such as lipid to protein ratio,

protein secondary structure can be used in early diagnosis of diabetes which will also stimulate the development of patient monitoring devices having particularly importance in detection of metabolic disorders. In conclusion, this current study provides new insight on the etiological and therapeutic aspects of diabetes mellitus.

CHAPTER 5

CONCLUSION

The results of the present study indicated that significant alterations occurred in EDL and SOL skeletal muscle tissues in STZ-induced type I diabetes.

The detailed examination of the FTIR spectra revealed the following observations:

There was a considerable decrease in both lipid and protein content of skeletal muscles, and both decreases were more easily observed for SOL muscle. It was also demonstrated for the first time in this current study that the decrease in lipid content was more remarkable when compared with the decrease in protein content. The decrease in lipid content suggested that lipolysis was increased in diabetic muscles. While, the decrease in protein content showed that either protein breakdown was increased in skeletal muscles, or skeletal muscle protein synthesis was decreased. The observed changes in protein structure and conformation were reported in this current study for the first time.

Glycogen level was lower in diabetic skeletal muscle tissues, especially in SOL muscles. In addition hydrogen bonding capacity of glycogen or proteins was decreased in diabetes.

In diabetes, muscle membrane lipids were more ordered when compared to control membranes, and this increase in order was more pronounced in EDL muscle. The amount of unsaturated lipids decreased in diabetic tissues indicating the increased lipid peroxidation. Lipid peroxidation was found to be higher in SOL muscles which rely on oxidative metabolism. On the other hand, the disordering effect of diabetes was observed for unsaturated lipids in SOL muscle, but not in EDL muscle.

Diabetes caused a decrease in the content of nucleic acids, especially RNA, and phospholipids in the membrane structures of skeletal muscles. It also caused a change in DNA and RNA conformation, possibly by increasing the effect of hydrogen bonding in the DNA and RNA backbones.

The disordering effect of diabetes for unsaturated lipids, change in DNA and RNA conformation, increase in hydrogen bonding of the DNA and RNA backbones were investigated for the first time in the present study.

In conclusion, in all of the spectral parameters investigated SOL muscle, which is composed of a high content of type I fibers, was found to be more severely affected from diabetes. This study was first to demonstrate the effect of type I diabetes on the whole macromolecular content of skeletal muscle tissues, simultaneously. Moreover, it gives new insights to clinical studies for the development of new therapies and drugs for the treatment of diabetes.

REFERENCES

Altomare, E., Vendemiale, G., Chicco, D., Procacci, V., Cirelli, F., (1992). "Increased lipid peroxidation in type II poorly controlled diabetic patients", Diabetes Metab., 18:264–271.

Ariano M.A., Armstrong R.B., Edgerton V.R., (1973). "Hindlimb muscle fiber populations of five animals", J. Histochem., 21:51–55.

Aragno, M., Mastrocola, R., Catalano, M.G., Brignardello, E., Danni, O., Boccuzzi, G., (2004). "Oxidative stress impairs skeletal muscle repair in diabetic rats", Diabetes, 53:1082–1088.

Armstrong, R.B., Gollnick P.D. and Ianuzzo, C.D., (1975). "Histochemical properties of skeletal muscle fibers in streptozotocin – diabetic rats". Cell Tiss. Res., 162: 387-394.

Armstrong, R.B., and Ianuzzo, C.D., (1977). "Compensatory hypertrophy of skeletal muscle fibers in streptozotocin-diabetic rats", Cell Tiss. Res., 181: 255-266.

Arrondo, J.L.R., Goni, F.M. and Macarulla, J.M., (1984). "Infrared spectroscopy of phosphatidylcholines in aqueous suspension a study of the phosphate group vibrations", BBA, 794, 165-168.

Arrondo, J.R., Muga, A., Castresa, J., and Goni, R. M., (1993). "Quantative Studies of the Structure of Proteins in Solution by Fourier Transfrom Infrared Spectroscopy", Progress. Biophys. Acta., 468:63-72.

Baldwin, K.M., Reitman J.S., Terjung, R.L., Winder, W.W., Holloszy, J.O., (1973). "Substrate depletion in different types of muscle and liver during prolonged running", Am. J. Physiol., 225:1045-1050.

Banyay, M., Sarkar, M., Graslund, A., (2003). "A library of IR bands of nucleic acids in solution", Biophysical Chemistry, 104: 477–488.

Baynes, J.W., (1991). "Role of oxidative stress in development of complications in Diabetes", Diabetes 40:405–412.

Bennet, W. M., Connacher, A. A., Smith, K., Jung, R. T. & Rennie, M. J., (1990). "Inability to stimulate skeletal muscle or whole body protein synthesis in type 1 (insulin-dependent) diabetic patients by insulin-plus-glucose during amino acid infusion: studies of incorporation and turnover of tracer L-[1-13C] leucine", Diabetologia, 33: 43–51.

Bernroider, E., Brehm, A., Krssak, M., Anderwald, C., Trajanoski, Z., Cline, G., Shulman, G.I., Roden, M., (2005). "The role of intramyocellular lipids during hypoglycemia in patients with intensively treated type 1 diabetes", J. Clin. Endocrinol. Metab., 90: 5559-5565.

Bizeau, M.E., Salano, J.M., and Jeffrey, R., (2000). "Menhaden oil feeding increases lypolysis without changing plasma membrane order in isolated rat adipocytes", Nutrition Research, 20(11): 1633-1644.

Block, N.E., Komori, K., Robinson, K.A., Dutton, S.L., Lam, C.F. and Buse, M.G., (1991). "Diabetes-associated impairment of hepatic insulin receptor tyrosine kinase activity: a study of mechanisms", Endocrinology 128:312-322.

Boyar, H. and Severcan, F., (1997). "Oestrogen-phopholipid membrane interactions: An FTIR study", J. Mol. Structure, 408-409, 269-272.

Burke, R.E., Levine, D.N., Tsairis, P., (1975). "Physiological types and histochemical profiles in motor units of cat gastrocnemius", J. Physiol., 234: 732-748.

Cael, J.J., Koenig, J.L., Blackwell, J., (1973). "Infrared and raman spectroscopy of carbohydrates. 3. Raman spectra of the polymorphic forms of amylase", Carbohydr. Res., 29(1):123-34.

Cakmak, G., Togan, I., Severcan, F., (2006). "17β-Estradiol induced compositional, structural and functional changes in rainbow trout liver, revealed by FT-IR spectroscopy: A comparative study with nonylphenol", Aquatic Toxicology, 77: 53–63.

Calore, E.E., Fratini, P. and Correa H., (2002). "Morphometric evalution of muscle fiber types in different skeletal muscle of rats", J. SubMicrosc, Cytol. Pathol., 34(4): 403-407.

Camacho, N.P., West, P., Torzilli, P.A., Mendelsohn, R., (2001). "FTIR microscopic imaging of collagen and proteoglycan in bovine cartilage", Biopolymers (Biospectroscopy), 62: 1–8.

Campenau, L., Campenau, S., Ionescu, M.D., (1971). "Ultrastructural alterations of the striated muscle cells in diabetes mellitus", Acta Diabet. Lat., 8: 680-710.

Carpenter, J.F., Crowe, J.H., (1989). "An infrared spectroscopic study of the interactions of carbohydrates with dried proteins", Biochemistry, 28(9):3916-22.

Casal, H. L. and Mantsch, H. H., (1984). "Polymorphic phase behavior of phospholipid membranes", BBA, 779, 381-401.

Chang, M.C., Tanaka, J., (2002). "FT-IR study for hydroxyapatite/collagen nanocomposite cross-linked by glutaraldehyde", Biomaterials, 23: 4811–4818.

Charlton, M., Nair, K.S., (1998). "Protein Metabolism in Insulin-Dependent Diabetes Mellitus", J. Nutr., 128: 323S–327S.

Chao, T.T., Ianuzzo C.D., Armstrong R.B.; Albright J.T. and Anapolle S.E., (1976). "Ultrastructural alterations in skeletal muscle fibers of streptozotocin-diabetic rats", Cell Tiss. Res., 168, 239-246.

Chiriboga, L., Yee, H., Diem, M., (2000). "Infrared spectroscopy of human cells and tissues. Part VI: A comparative study of histopathology and infrared microspectroscopy of normal, cirrhotic, and cancerous liver tissue", Appl. Spectrosc., 54: 1-8.

Ci, X. Y., Gao, T. Y., Feng, J. and Guo, Z. Q., (1999). "Fourier transform infrared characterization of human breast tissue: Implications for breast cancer diagnosis", Applied Spectroscopy, 53:312-315.

Colthup, N. B., Daly, L. H. and Wiberley, S. E., (1975). Introduction to infrared and raman spectroscopy, New York: Academic Press.

Curtis, M.T., Gilfor, D., Farber, J.L., (1984). "Lipid peroxidation increases the molecular order of microsomal membranes", Arch. Biochem. Biophys. 235:644–649.

Çakmak, G., Togan, I., Uguz, C., Severcan, F., (2003). "FT-IR spectroscopic analysis of rainbow trout liver exposed to nonylphenol", Appl. Spec. 57:835–841.

DeFronzo, R.A., Jacot, E., Jequier, E., Maeder, E., Wahren, J., Felber, J.P., (1981). The effect of insulin on the disposal of intravenous glucose, Diabetes, 30:1000-1007.

DeFronzo, R.A., Sherwin, R.S., Kraemer, N., (1987). "Effect of physical training on insulin action and obesity", Diabetes, 36: 1379–1385.

Delp, M.D., Duan, C., (1996). "Composition and size of type I, IIA, IID/X, and IIB fibers and citrate synthase activity of rat muscle", J. Appl. Physiol,. 80(1):261-270.

Denne,S.C., Liechty, E.A., Liu,Y.M., Brechtel,G., Baron, A.D., (1991). "Proteolysis in skeletal muscle and whole body in response to euglycemic hyperinsulinemia in normal adults", A. J. Physiol., 261: E809–E814.

Diem, M., (1993). Introduction to modern vibrational spectroscopy, John Wiley & Sons, USA.

Diem, M., Boydston-White, S., Chiriboga, L., (1999). "Infrared spectroscopy of cells and tissues: shining light onto a novel subject", Applied Spectroscopy, 53, 148A-161A.

Dousseau, F, and Pezolet, M., (1990). “Determination of the secondary structure content of proteins in aqueous solutions from their amide I and amide II infrared bands. Comparison between classical and partial least-squares methods?”, Biochemistry, 29: 8771-8779.

Dovbeshko, G. I., Gridina, N. Y., Kruglova, E. B. and Pashchuk, O. P., (2000). “FTIR spectroscopy studies of nucleic acid damage”, Talanta, 53, 233-246.

Ebeling, P., Essen-Gustavsson, B., Tuominen, J.A., Koivisto, V.A., (1998). “Intramuscular triglyceride content is increased in IDDM”, Diabetologia, 41:111–115.

Engel, W.K., (1962). “The essentiality of histo- and cytochemical studies of skeletal muscle in the investigation of neuromuscular disease”, Neurology (Minneapolis), 12: 778-794.

Esterbauer, H.., Schaur, R.J., Zollner, H., (1991). “Chemistry and biochemistry of 4-hydroxynonenal, malonaldehyde and related aldehydes”, Free Radic. Biol. Med., 11:81-128.

Freifelder, D., (1982). Physical Chemistry. Applications to biochemistry and molecular biology, Freeman, W. H. (Ed), New York.

Garrett, W.E., Mumma, M., Lucaveche, C.L., (1983). “Ultrastructural differences in human skeletal muscle fiber types”, Orthopedic Clinics of North America, 14(2): 413-425.

Garvey, W.T., Hueckstead, T.P. and Birnbaum, M.J., (1989). “Pretranslational suppression of an insulin responsive glucose transporter in rats with diabetes mellitus”, Science (Wash D.C.), 245:60-63.

Glatz, J.F.C., Bonen, A., Luiken, J.J.F.P., (2002). “Exercise and insulin increase muscle fatty acid uptake by recruiting putative fatty acid transporters to the sarcolemma”, Curr. Opin. Clin. Nutr. Metab. Care, 5: 365-370.

Green K., Brand, M.D., Murphy, M.P., (2004). “Prevention of mitochondrial oxidative damage as a therapeutic strategy in diabetes”. Diabetes, 53(Suppl. 1):S110-S118.

Greisheimer, E.M. and Wiedeman, M.P., (1972). Physiologyand anatomy, 9th Ed., J.B. Lippincott Company, Washington.

Griffiths, P. R. and De Haseth, J. A., (1986). Fourier transform infrared spectrometry. NewYork: Wiley.

Golay, A., DeFronzo, R.A., Ferrannini, E., (1998). “Oxidative and non-oxidative glucose metabolism in non-obese type 2 (non-insulin-dependent) diabetic patients”. Diabetologia, 31: 585–591.

Gollnick, P.D., Piehl, K., Saltin, B., (1974). "Selective glycogen depletion pattern in human muscle fibers after exercise of varying intensity and at varying pedaling rates", J. Physiol., 241: 45-57.

Goodpaster, B.H., Thaete, F.L., Simoneau, J.A., Kelley, D.E., (1997). "Subcutaneous abdominal fat and thigh muscle composition predict insulin sensitivity independently of visceral fat", Diabetes, 46:1579-1585.

Goodpaster, B.H., He, J., Watkins, S., Kelley, D.E., (2001). "Skeletal muscle lipid content and insulin resistance: evidence for a paradox in endurance-trained athletes", J Clin Endocrinol Metab, 86:5755-5761.

Goodpaster, B.H., and Wolf, D., (2004). "Skeletal muscle lipid accumulation in obesity, insulin resistance, and type 2 diabetes", Pediatric Diabetes, 5: 219-226.

Goodpaster, B.H., and Brown, N.F., (2005). "Skeletal muscle lipid and its association with insulin resistance: what is the role for exercise?", Exerc. Sport Sci. Rev., 33(3):150-154.

Gough, K.M., Zelinski, D., Wiens, R., Rak, M., Dixon, I.M.C., (2003). "Fourier transform infrared evaluation of microscopic scarring in the cardiomyopathic heart: Effect of chronic AT1 suppression", Analytical Biochemistry, 316 232-242.

Gunnarson, R., Berne, C. and Hellerström, C., (1974). "Cytotoxic effects of streptozotrocin and N-nitrosomethylurea on the pancreatic β cells with special regard to the role of nicotinamideadenine dinucleotide", Biochem. J., 140:487-494.

Hagström-Toft, E., Qvisth, V., Nennesmo, I., Ryden, M., Bolinder, H., Enoksson, S., Bolinder, J., Arner, P., (2002). "Marked heterogeneity of human skeletal muscle lipolysis at rest", Diabetes, 51:3376–3383.

Hall, J.C., Sordahl, L.A., Stefko, P.L., (1960). "The effect of insulin on oxidative
phosphorylation in normal and diabetic mitochondria", J. Biol. Chem., 235: 1536-1539.

Halliwell, B., Gutteridge, J.M.C., (1989), "Free radicals in biology and medicine", 2nd Ed, Clarendon, Oxford Science Publishers, UK.

Haris, P. I. and Severcan F., (1999). "FTIR spectroscopic characterization of protein structure in aqueous and non-aqueous media", J. Molecular Catalysis B: Enzymatic, 7, 207-221.

Haris, P. I. and Chapman, D., (1996). Fourier transform infrared spectroscopic studies of biomembranes systems, Infrared Spectroscopy of Biomolecules, Wiley-Liss, Inc., USA, 239-278.

He, J., Watkins, S. and Kelley, D.E., (2001). "Skeletal muscle lipid content and oxidative enzyme activity in relation to muscle fiber type in type 2 diabetes and obesity", Diabetes, 50: 817- 823.

He, J., and Kelley, D.E., (2004). "Muscle glycogen content in type 2 diabetes mellitus", Am. J. Physiol. Endocrinol. Metab., 287:1002-1007.

Hebel, R., and Stromberg, M.W., (1976). Anatomy of the laboratory rat, The Williams and Wilkins Company, Baltimore.

Helm, D., Labischinski, H., Schallehn, G., Naumann, D., (1991). Classification and identification of bacteria by Fourier-transform infrared spectroscopy, J. Gen. Microbiol., 137:69–79.

Hopp, J.F., and Palmer, W.K., (1991). "Effect of glucose and insulin on triacylglycerol metabolism in isolated normal and diabetic skeletal muscle", Metabolism, 40(3): 223- 225.

Jackson, M., Ramjiawan, B., Hewko, M., and Mantsch, H. H., (1998). "Infrared microscopic functional group mapping and spectral clustering analysis of hypercholosterolomic rabbit liver", Cell. Mol. Biol., 44(1): 89-98.

Jacob, S., Hauer, B., Becker, R., Artzner, S., Grauer, P., Löblein, K., Nielsen, M., Renn, W., Rett, K., Wahl, H.-G., Stumvoll, M., Häring, H.-U., (1999). "Lipolysis in skeletal muscle is rapidly regulated by low physiological doses of insulin", Diabetologia, 42: 1171-1174.

Jamin, N., Dumas, P., Moncuit, J., Fridman, W., Teillaud, J., Carr, L. G., and Williams, G. P., (1998). "Highly resolved chemical imaging of living cells by using synchrotron infrared microspectroscopy", Applied Biological Sciences, 95(9): 4837-4840.

Kayalı, R., Cakatay, U., Telci, A., Akçay, T., Sivas, A., Altuğ, T., (2004). "Decrease in mitochondrial oxidative protein damage parameters in the streptozotocin- diabetic rat", Diabetes Metab. Res. Rev., 20: 315–321.

Katz, E.B., Burcelin, R., Tsao, T.S., Stenbit, A.E., Charron, M.J., (1996). "The metabolic consequences of altered glucose transporter expression in transgenic mice", J. Mol. Med., 74: 639-652.

Kelley, D.E., Goodpaster, B.H., (2001). "Skeletal muscle triglyceride, An aspect of regional adiposity and insulin resistance", Diabetes Care, 24 (5): 933-941.

Kern M., Wells, J.A., Stephens, J.M., Elton, C.W., Friedman, J.E., Tapscott, E.B., Pekala, P.H., Dohm, G.L., (1990). "Insulin responsiveness in skeletal muscle is determined by glucose transporter (Glut4) protein level". Biochem. J., 270:397-400.

Kinder, R., Ziegler, C., Wessels, J.M., (1997). "γ-Irradiation and UV-C light-induced lipid peroxidation: A Fourier transform-infrared absorption spectroscopic study", Int. J. Radiat. Biol., 71(5): 561-571.

Kneipp, J., Lasch, P., Baldauf, E., Beekes, M. and Naumann, D., (2000). "Detection of pathological molecular alterations in scrapie-infected hamster brain by Fourier transform infrared (FT-IR) spectroscopy", BBA, 1501, 189-199.

Knip, M., Akerblom, H.K., (1998). "IDDM prevention trials in progress--a critical assessment", J. Pediatr. Endocrinol. Metab., Suppl 2:371-7.

Korkmaz, F., and Severcan, F., (2005). "Effect of progesterone on DPPC membrane: Evidence for lateral phase separation and inverse action in lipid dynamics", Arch. Biochem. Biophys., 440: 141–147.

Kumar, V., Cotran, R.S., and Robbins, S.L., (1997). Basic Pathology, 6th Ed., W.B. Saunders Company, Philedelphia.

Lamba, Om P., Lal, S., Yappert, M.C., Lou, M.F. and Borchman, D., (1991). "Spectroscopic detection of lipid peroxidation products and structural changes in a sphingomyelin model system", BBA, 1081, 181-187.

Leary, S.C., Lyons, C.N., Rosenberger, A.G., Ballantyne, J.S., Stillman, J., Moyes, C.D., (2003). "Fiber-type differences in muscle mitochondrial profiles", Am. J. Physiol. Regulatory Integrative Comp. Physiol., 285:817-826.

Lehti, T.M., Silvennoinen, M., Kivela, R., Kainulainen, H., Komulainen, J., (2006). "Effects of streptozotocin-induced diabetes and physical training on gene expression of extracellular matrix proteins in mouse skeletal muscle", Am. J. Physiol. Endocrinol. Metab., 290(5):E900-7.

Levin, G., Cogan, U., Levy, Y., Mokady, S., (1990). "Riboflavin deficiency and the function and fluidity of rat erythrocyte membranes", J. Nutr. 120:857–861.

Liquier J. and Taillandier, E., (1996). Infrared spectroscopy of nucleic acids, Infrared Spectroscopy of Biomolecules, Wiley-Liss, Inc., USA, 131-158, 1996.

Lithell, H., Lindgarde, F., Hellsing, K., Lundqvist, G., Nygaard, E., Vessby, B., Saltin, B., (1981). "Body weight, skeletal muscle morphology, and enzyme activities in relation to fasting serum insulin concentration and glucose tolerance in 48-year-old men". Diabetes, 30:19-25.

Lithell, H. and Berne, C., (1991). Diabetogenic Drugs. Pharmacology of Diabetes: Present Practice and Future Perspectives, 3:57-74. Walter de Gruyter, Berlin.

Liu, K.Z., Bose, R., Mantsch, H.H., (2002). "Infrared spectroscopic study of diabetic platelets", Vibrational Spectroscopy, 28: 131–136.

Lopez-Garcia, F., Villian, J., and Gomez-Fernandez, J.C., (1993). "Infrared spectroscopic studies of the interaction of diacylglycerols with phosphatidylcerol, phosphatidylserin in the presence of calcium". Biochim Biophys Acta, 1169: 264-272.

Luzi, L., Castellino, P., Simonson, D.C., Petrides, A.S., DeFronzo, R.A., (1990). "Leucine metabolism in IDDM. Role of insulin and substrate availability", Diabetes, 39: 38–48.

Lyman, D.J., and Murray-Wijelath, J., (1999). "Vacular graft healing: I.FTIR analysis of a implant model for studying the healing of a vascular graft". J. Biomed. Mater. Res. (Appl. Biomater.), 48; 172-186.

Lyman, D.J., Murray–Wijelath, J., Ambrad–Chalela, E., Wijelath, E.S., (2001). "Vascular graft healing. ii. ftir analysis of polyester graft samples from implanted bi-grafts", J. Biomed. Mater. Res. (Appl. Biomater.), 58: 221–237.

Mantsch, H.H., (1984). "Biological application of Fourier Transform Infrared Spectroscopy: A study of phase transitions in biomembranes". J. Mol. Strucutre, 113: 201-212.

Malenfant, P., Joanisse, D.R., Theriault R., Goodpaster, B.H., Kelley, D.E. and Simoneau, J-A., (2001). "Fat content in individual muscle fibers of lean and obese subjects". International Journal of Obesity, 25: 1316-1321.

Magnuson, M.A., Andreone, T.L., Printz, R.L., Koch, S. and Granner, D.K., (1989). "Rat glucokinase gene:structure and regulation by insulin". Proc. Natl. Acad. Sci. USA, 86:4838-4842.

Mandrup-Poulsen, T., (1990). "Cytokine-mediated beta-cell destruction: the molecular effector mechanism causing IDDM?", J. Autoimmun. Suppl., 1:121-122.

Manoharan, R., Baraga, J.J., Rava, R.P., Dasari, R.R., Fitzmaurice, M. and Feld, M.S., (1993). "Biochemical analysis and mapping of atherosclerotic human artery using FTIR microspectroscopy". Atherosclerosis, 103:181-193.

McAinch, A.J., Lee, J.S., Bruce, C.R., Tunstall, R.J., Hawley, J.A., (2003). "Cameron-Smith, D., Dietary regulation of fat oxidative gene expression in different skeletal muscle fiber types", Obesity Research, 11 (12): 1471-1479.

McArdle, W.D., Katch, F.I., Katch, V.L., (2001). Exercise Physiology, Energy, Nutrition and Human Performance, 5th Ed., Lippincott Williams and Wilkins, Washington.

Mendelsohn, R. and Mantsch, H. H., (1986). Fourier transform infrared studies of lipid-protein interaction, Progress in Protein-Lipid Interactions, Volume 2, Elsevier Science Publishers, Netherlands, 103-147.

Moller-Loswick, A.C., Zachrisson, H., Hyltander, A., Korner, U., Matthews, D. E., Lundholm, K., (1994). "Insulin selectively attenuates breakdown of nonmyofibrillar proteins in peripheral tissues of normal men". Am. J. Physiol., 266: E645–E652.

Moore, K.P., Darley-Usmar, V., Morrow, J., Roberts, L.J., (1995). "Formation of F2-isoprostanes during oxidation of human low-density lipoprotein and plasma by peroxynitrite", Circ. Res., 77:335-341.

Moustaid, N., Beyer, R. S. and Sul, H. S., (1994). "Identification of an insulin response element in the fatty acid synthase promoter". J. Biol. Chem., 269:5629-5634.

Melin, A., Perromat, A., and Deleris, G., (2000). "Pharmacologic Application of Fourier Transform IR Spectroscopy: In vivo Toxicity of Carbon tetrachloride on rat liver", Biopolymers (Biospectroscopy), 57:160-168.

Nara, M., Okazaki, M., Kagi, H., (2002). "Infrared study of human serum verylow-density and low-density lipoproteins. Implication of esterified lipid C=O stretching bands for characterizing lipoproteins". Chem. Phys. Lipids, 117: 1–6.

Nemeth, P. and Pette, D., (1981). "Succinate dehydrogenase activity in fibres classified by myosin ATPase in three hind limb muscles of rat", J. Physiol. (London), 320: 73-80.

Netto, L.E., Kowaltowski, A.J., Castilho, R.F., Vercesi, A.E., (2002). "Thiol enzymes protecting mitochondria against oxidative damage", Methods Enzymol., 348:260–270.

Nilsson, A., Holmgren, A., Lindblom, G., (1991). "Fourier-Transform infrared spectroscopy study of dioleoylphosphatidylcholine and monooleoylglycerol in lamellar and cubic liquid crystalst", Biochemistry, 30: 2126-2133.

Niranjan, T.G., Krishnakantha, T.P., (2000). "Membrane changes in rat erythrocyte ghosts on ghee feeding", Mol. Cell. Biochem. 204:57–63.

Oakes, N.D., Bell, K.S., Furler, S.M., Camilleri, S., Saha, A.K., Ruderman N.B., Chisholm, D.J., Kraegen, E.W., (1997). "Diet-induced muscle insulin resistance in rats is ameliorated by acute dietary lipid withdrawal or a single bout of exercise: parallel relationship between insulin stimulation of glucose uptake and suppression of long-chain fatty acyl-CoA". Diabetes, 46:983-988.

O'Brien, R. M., Lucas, P. C., Forest, C., Magnuson, M. A., and Granner, D. K., (1990). "Identification of asequence in the PEPCK gene that mediates a negative effect of insulin on transcription". Science 249:533-537.

O'Brien, R. M. and Granner, D. K., (1996). "Regulation of gene expression by insulin". Physiol. Rev., 76:1109-1161.

Okumura, N., Hashida-Okumura, A., Kita, K., Matsubae, M., Matsubara, T., Takao, T., Nagai, K., (2005). "Proteomic analysis of slow- and fast-twitch skeletal muscles", Proteomics, 5: 2896–2906.

Özturk, Y., Altan, V.M., and Yildizoglu-Ari, N., (1997). "Effect of experimental diabetes and insulin on smooth muscle cell functions", Pharmacological Reviews 48 (1):1-44.

Pacy, P.J., Bannister, P.A., Halliday, D., (1991). "Influence of insulin on leucine
kinetics in the whole body and across the forearm in post-absorptive insulin dependent diabetic (type 1) patients", Diabetes Res., 18: 155–162.

Pevsner, A., Diem, M., (2003). "IR spectroscopic studies of major cellular components. III. Hydration of protein, nucleic acid, and phospholipid films", Biopolymers, 72(4):282-9.

Perseghin, G., Lattuada, G., Danna, M., Sereni, L.P., Maffi, P., De Cobelli, F., Battezzati, A., Secchi, A., Del Maschio, A., Luzi, L., (2003). "Insulin resistance, intramyocellular lipid content, and plasma adiponectin in patients with type 1 diabetes". Am. J. Physiol., 285:E1174–E1181.

Perseghin, G., Lattuada, De Cobelli, F., Esposito, A., Costantino, F., Canu, T., Scifo, P., De Taddeo, F., Maffi, P., Secchi, A., Del Maschio, A., Luzi, L., (2005). "Reduced intrahepatic fat content is associated with increased whole-body lipid oxidation in patients with type 1 diabetes", Diabetologia, 48: 2615-2621.

Rabinovitch, A. and Baquerizo, H., (1990). "Immunological mechanisms of pancreatic β-cell destruction:effects of cytokines", J. Autoimmun., 3:85.

Ramlal, T., Rasgoti, S., Vranic, M, Klip, A., (1989). "Decrease in glucose transporter number in skeletal muscle of mildly diabetic (streptozotocin-treated) rats", Endocrinology (Baltimore), 125:890-897.

Rana, F.R., Sultany, C.M. and Blazyk, J., (1990). "Interactions between Salmonella typhimurium lipopolysaccharide and the antimicrobial peptide, magainin 2 amide", FEBS Letters, 261, 2, 464-467.

Raudenkolb, S., Hübner, W., Rettig, W., Wartewig,S., Neubert, R.H.H., (2003). "Polymorphism of ceramide 3. Part 1: an investigation focused on the head group of N octadecanoylphytosphingosine", Chem. Phys. Lipids, 123: 9-17.

Rigas, B., Morgellot, S., Goldman, I.S., Wong, P.T.T., (1990). "Human colorectal cancers display abnormal Fourier-transform infrared spectra", Proc. Nati. Acad. Sci. , 87: 8140-8144.

Spassov, S., Beekes M., Naumann, D., (2006). "Structural differences between TSEs strains investigated by FT-IR spectroscopy", Biochimica et Biophysica Acta, 1760: 1138–1149.

Schiaffino S. and Reggiani C., (1991). "Molecular diversity of myofibrillar proteins: gene regulation and functional significance", Physiol. Rev., 76 (2): 371-423.

Schultz, C. and Naumann, D., (1991). "In vivo study of the state of order of the membranes of Gram-negative bacteria by Fourier-transform infrared spectroscopy (FT-IR)", FEBS Letters, 294, 43-46.

Severcan, F., Kazancı, N., Baykal, U., Süzer, S., (1995). "IR and turbidity studies of vitamin E-cholesterol-phospholipid membrane interactions", Bioscience Reports, 15 (4) 221-229.

Severcan, F., (1997). "Vitamin E decreases the order of the phospholipid model membranes in the gel phase: An FTIR study". Bioscience Reports, 17: 231-235.

Severcan, F., Yazıcı, Z., Güray, T., (1999). "Interaction of vitamin E-acetate with human erythrocyte membranes", Chem. Phys. Lipids 101:176-177.

Severcan, F., Toyran, N., Kaptan, N. and Turan, B., (2000). "Fourier transform infrared study of diabetes on rat liver and heart tissues in the C-H region", Talanta, 53, 55-59.

Severcan, F., Kaptan, N., Turan, B., (2003). "Fourier transform infrared spectroscopic studies of diabetic rat heart crude membranes", Spectroscopy, 17: 569–577 569.

Severcan, F., Gorgulu, G., Gorgulu, S.T., Guray, T., (2005). "Rapid monitoring of diabetes-induced lipid peroxidation by Fourier transform infrared spectroscopy: Evidence from rat liver microsomal membranes", Anal. Biochem., 339: 36–40.

Shepherd, P.R., Navé, B.T. and Siddle, K., (1995). "Insulin stimulation of glycogen synthesis and glycogen synthase activity is blocked by wortmannin and rapamycin in 3T3-L1 adipocytes: evidence for the involvement of phosphoinositide-3kinase and p70 ribosomal protein-S6 kinase". Biochem J., 305:25-28.

Shier, D., Butler, J., Lewis, R., (1996). Hole's human anatomy and phsiology, Wm. C. Brown Publishers, Dubuque.

Short, J.M., Wynshaw-Boris, A., Short, H.P. and Hanson, R.W., (1986). "Characterization of the phosphoenolpyruvate carboxykinase (GTP) promoter-regulatory region". J. Biol. Chem., 261:9721-9726.

Sills, R.H., Moore, D.J. and Mendelsohn, R., (1994). "Erythrocyte peroxidation: quantitation by fourier transform infrared spectroscopy". Analytical Biochemistry 218: 118-123.

Slieker, L.J., Roberts, E.F., Shaw, W.N. and Johnson, W.T., (1990). "Effect of streptozotocin-induced diabetes on insulin-receptor tyrosine kinase activity in obese zucker rats". Diabetes 39: 619-625.

Smith, G.C.M., and Jackson, S.P., (1999). "The DNA dependant protein kinase", Genes Dev. 13, 916-934.

Stapleton, S.R., Mitchell, D.A., Salati, L.M. and Goodridge, A.G., (1990). "Triiodothyronine stimulates transcription of the fatty acid synthase gene in chick embryo hepatocytes in culture". J. Biol. Chem., 265:18442-18446.

Stapleton, S.R., (2000). "Selenium: an insulin-mimetic". Cellul. Molec. Life Sci., 57:1874-1879.

Stearns, S.B., Tepperman, H.M., Tepperman, J., (1979). "Studies on the utilization and mobilization of lipid in skeletal muscles from streptozotocin-diabetic and control rats", J. Lipid Res., 20: 654-662.

Steele, D., (1971). The Interpretation of Vibrational Spectra, William Clowes & Sons Lim., Great Britain.

Stuart, B., (1997). Biological Applications of Infrared Spectroscopy. John Wiley and Sons, Ltd., England.

Strout, H.V., Vicario, P.P., Biswas, C., Saperstein, R., Brady, E.J., Pilch, P.F. and Berger, J., (1990). "Vanadate treatment of streptozotocin diabetic rats restores expression of the insulin-responsive glucose transporter in skeletal muscle". Endocrinology, 126:2728-2732.

Suzuki, H., Jang, H.G. and Rhim J.H., (1999). "Effect of oxidized fish oil and α-tocopherol on the peroxidation of erythrocyte membrane phospholipids in rats", Food and Chemical Toxicology, 37:509-513.

Szalontai, B., Nishiyama, Y., Gombos, Z., and Murata, N., (2000). "Membrane dynamics as seen by Fourier Transform Infrared Spectroscopy in a cyanobacterium, synechocystis PCC 6803. The effects of lipid unsaturation and the protein-to-lipid ratio", Biochim. Biophys. Acta, 1509; 409-419.

Taillandier, E., and Liquier, J., (1992). "Infrared spectroscopy of DNA", Methods Enzymol., 211:307–335.

Takahashi, H., French, S. M., and Wong, P. T. T., (1991). "Alterations in hepatic lipids and proteins by Chronic ethanol Intake: A highpressure fourier transform Infrared spectroscopic study on alcoholic liver disease in the rat alcohol". Clin. Exp. Res., 15(2): 219-223.

Tomlinson, K. C., Gardiner, S. M., Hebden, R. A. and Bennett, T., (1992). "Functional consequences of streptozotocin-induced diabetes mellitus, with particular reference to the cardiovascular system". Pharmacol Rev., 44:103-150.

Toyran, N., and Severcan, F., (2003). "Competitive effect of vitamin D2 and Ca^{2+} on phospholipids model membranes: an FTIR study", Chem. Phys. Lipids, 123:165-176.

Toyran, N., Zorlu, F., Dönmez, G., Öğe, K., Severcan, F., (2004). "Chronic hypoperfusion alters the content and structure of proteins and lipids of rat brain homogenates: A Fourier transform infrared spectroscopy study", Eur. Biophys. J., 33: 549–554.

Toyran, N., Lasch, P., Naumann, D., Turan, B., Severcan, F., (2006). "Early alterations in myocardia and vessels of the diabetic rat heart: an FTIR microspectroscopic study", Biochem J., 397(3):427-36.

Tsuboi, M., (1969). Application of infrared spectroscopy to structure studies of nucleic acids, Applied Spectroscopy Reviews, Dekker, New York, pp. 45–90.

van Loon, L.J.C., Koopman, R., Manders, R., van der Weegen, W., van Kranenburg, G.P., Keizer, H.A., (2004). „Intramyocellular lipid content in type 2 diabetes patients compared with overweight sedentary men and highly trained endurance athletes", Am. J. Physiol. Endocrinol. Metab., 287: E558–E565.

Venojärvi, M., Puhke R., Hämäläinen, H., Marniemi, J., Rastas M., Rusko, H., Nuutila, P., Hänninen, O. and Aunola S., (2005). "Role of skeletal muscle-fibre type in regulation of glucose metabolism in middle-aged subjects with impaired glucose tolerance during a long term exercise and dietary intervention". Diabetes, Obesity and Metabolism, 7: 745-754.

Voortman, G., Gerrits, J., Altavilla, M., Henning, M., Van Bergeijk, L., Hessels, J., (2002). "Quantitative determination of faecal fatty acids and triglycerides by Fourier transform infrared analysis with a sodium chloride transmission flow cell". Clin. Chem. Lab. Med., 40:795–798.

Wagle, A., Jivraj, S., Garlock, G. and Stapleton, S. R., (1998). "Insulin regulation of glucose-6-phosphate dehydrogenase gene expression is rapamycin sensitive and requires phosphatidylinositol 3-kinase". J. Biol. Chem., 273:14968-14974.

Wang, J., Chi, C., Lin, S., and Chern, Y., (1997). "Conformational changes in gastric carcinoma cell membrane protein correlated to cell viability after treatment with adamantyl maleimide", Anticancer Research, 17: 3473-3478.

West, I.C., (2000). "Radicals and oxidative stress", Diabetic Medicine, 17: 171-180.

West, P.A., Bostrom, P.G., Torzilli, P.A., and Camacho, N.P., (2004). "Fourier Transform Infrared Spectral analysis of degenerative cartilage: an infrared fiber optic probe and imaging study". Applied Spectroscopy, 58(4): 376-381.

Wolff, S.P., (1993), "Diabetes mellitus and free radicals. Free radicals, transition metals and oxidative stress in the etiology of diabetes mellitus and complications", Br. Med. Bull. 49: 642–652.

Wong, P.T.T., Wong, R.K., Caputo, T.A., Godwin, T.A., Rigas, B., (1991). "Infrared spectroscopy of exfoliated human cervical cells: Evidence of extensive structural changes during carcinogenesis", Proc. Nati. Acad. Sci., 88: 10988-10992.

Wool, I.B., Stirewalt, W.S., Kuhira, K., Low, R.B., Bailey, P., Oyer, D., (1968). "Hormones and metabolic function- Mode of action of insulin in the regulation of protein biosynthesis in muscle", Recent Progr. Hormone Res., 24: 139-208.

Yono, K., Ohoshima, S., Shimuzu, Y., Moriguchi, T. and Katayama, H., (1996). "Evaluation of glycogen level in human lung carcinoma tissues by an infrared spectroscopic method". Cancer Letters, 110:29-34.